

## Theory of Photoemission in Simple Metals\*

G. D. MAHAN†

*Institute of Theoretical Science and Department of Physics, University of Oregon, Eugene, Oregon 97403*

(Received 24 June 1970)

A theory of photoemission is presented in which all results are derived rigorously from first principles. It is shown how to calculate properly the external current of electrons, with the transmission at the surface done correctly. A new and rigorous formalism is derived for doing many-body calculations in photoemission. Extensive calculations are performed on the angular dependence of photoemission. It is shown that the angular anisotropy is interesting and significant. Numerous numerical examples are presented for the alkali metals.

### I. INTRODUCTION

Surprisingly few theoretical papers have been written on the theory of photoemission from simple metals. Most of the early work was concerned with the surface effect.<sup>1,2</sup> Of those concerned with the volume effect, most have treated the surface in an off-hand or *ad hoc* manner.<sup>3-6</sup> Nor has a method been yet presented which treats many-body effects in a satisfactory fashion. The present article discusses these problems in detail, and solves them rigorously. In addition, a detailed discussion is presented on the angular dependence of photoemission. It is shown that the electrons are emitted with conical distributions, and that a measurement of these cone angles will provide information on the band structure of the metal.<sup>7</sup>

Photoemission has often been interpreted as a three-step process: optical absorption, transport to the surface, and transmission through the surface.<sup>4</sup> Recent work has challenged this view, and instead treated photoemission as a scattering process.<sup>6-8</sup> Here one views the experiment as the sending in of photons, and the measuring of electrons which come out. One can think of the process in terms of wave packets, or alternately one can use the outgoing-wave formalism of ordinary scattering theory. The conversion of ingoing photons to outgoing electrons is just an inelastic scattering process. The absorption of the photon raises an electron to an excited state, after which the outgoing electron may leave the crystal. Before leaving the vicinity of the crystal, the electron may experience other scattering processes and therefore be in other intermediate states along the way. We show that the multiple scattering may be adequately described by a  $T$  matrix. One way of evaluating this  $T$  matrix is to insert a Green's function  $G_0(\mathbf{r}, \mathbf{r}')$  between each operator. The argument over whether these intermediate states are real or virtual is one of semantics.<sup>8</sup> For example, the free-electron Green's function in one dimension may be written as

$$G_0(z, z') = \int_{-\infty}^{\infty} \frac{dk}{2\pi} \frac{\exp[ik(z-z')]}{\epsilon_k - \epsilon - i\delta} \quad (1.1a)$$

or alternatively as

$$G_0(z, z') = (im/p) \exp(ip |z-z'|), \quad p = (2m\epsilon)^{1/2}. \quad (1.1b)$$

These two forms are identical. In case (1.1a) it appears as if the electron states are summed over, and no single state dominates. In (1.1b) it appears that the electron is in a single state. These two identical expressions have quite different "physical" interpretations. In photoemission we are also concerned with evaluating an expression such as (1.1a), but it must be modified to account for (a) the three dimensionality of the problem, (b) the influence of the surface on the wave functions, and (c) the influence of band structure on the electrons. In spite of these complications, for simple metals one can still express the Green's function in a simple form similar to (1.1b). So the controversy over whether the intermediate states are real or virtual has no substance, since that is just a question of whether one should use the type of form for the Green's functions (1.1a) or (1.1b).

The amplitude of the electron wave function outside the crystal may be obtained by selecting a particular component of this  $T$  matrix. Our approach has a formal resemblance to that of Ashcroft and Schaich,<sup>8</sup> but our results are presented in a different and simpler way. For example, we explicitly discuss how the band structure of the metal influences the intensity of external photoemission. Band structure influences not only the absorption of light, but also the subsequent transport and transmission of the electron.

Most of this article is concerned with predicting the angles at which the electrons are emitted. The angular dependence of photoemission has not been measured, but the experiments are now in progress.<sup>9</sup> Our calculations show that inside the crystal the electrons have a conical distribution. The external distributions are determined by how these cones of electrons are projected through the surface. For nearly free electrons, the internal distributions consist of high-intensity primary cones, centered along the directions of reciprocal-lattice vectors, and weak-intensity secondary cones. These latter cones are a consequence of the band structure: Since the Bloch functions are linear combinations of plane waves,

$$\psi_{\mathbf{k}}(\mathbf{r}) = e^{i\mathbf{k}\cdot\mathbf{r}} \left\{ 1 + \sum_{\mathbf{G} \neq 0} u_{\mathbf{k},\mathbf{G}} e^{i\mathbf{G}\cdot\mathbf{r}} \right\} \left\{ 1 + \sum_{\mathbf{G} \neq 0} u_{\mathbf{k},\mathbf{G}}^2 \right\}^{-1/2},$$

an electron created in the outgoing state  $\mathbf{k}$  has plane-

TABLE I. Parameters employed in preparing the tables and figures in this article. All values are energies in eV except the first column of lattice vector  $a$ . The potential  $V_0$  equals the work function  $\varphi$  plus the Fermi energy. The two values of  $V_0$  represent using  $E_{F0}$  and  $E_F$ , respectively.

	$a^a$	$E_G$	$\varphi^b$	$E_{F0}$	$\delta E_F$	$E_F$	$V_0$	$V_{111}$
Li	6.597	24.67	2.28	4.75	-1.42	3.33	7.03/5.61	1.37 <sup>a</sup>
Na	7.984	16.84	2.25	3.24	-0.06	3.18	5.49/5.43	0.23 <sup>c</sup>
K	9.874	11.01	2.24	2.12	-0.07	2.05	4.36/4.29	0.20 <sup>c</sup>

<sup>a</sup> F. S. Ham, Phys. Rev. **128**, 84 (1962); **128**, 2524 (1962).

<sup>b</sup> F. Seitz, *Modern Theory of Solids* (McGraw-Hill, New York, 1940).

<sup>c</sup> A. W. Overhauser, Phys. Rev. **156**, 844 (1967).

wave components going in the directions  $\mathbf{k}+\mathbf{G}$ . Each of these components creates an external distribution of electrons. The primary component  $\exp(i\mathbf{k}\cdot\mathbf{r})$  makes the primary cones. The other components make distributions which are only approximately conical shape. Another way to visualize the secondary cones is to observe that they arise from trying to match plane-wave functions outside the crystal to Bloch functions inside. Outside the crystal, many plane waves are needed to match to the internal Bloch function, and each of these external plane-wave components provides another direction for electrons to come out of the solid, and is the direction of another distribution of electrons.

Figure 1(a) shows the experimental arrangement we have in mind in doing the calculations. Light illuminates a sample of area  $\mathcal{A}$ , and the electrons are collected in a hemispherical cup. The angular measurement consists of determining how many go into each unit of solid angle  $d\Omega$ . Another possible experimental arrangement is shown in Fig. 1(b). Here a sample of infinite area is illuminated with light, and electrons are collected in an area  $\mathcal{A}$ . This geometry will yield the same results as the total hemispherical method of Fig. 1(a). We make this remark because most experiments use the configuration in Fig. 1(a), while some of the theoreticians have calculated for the geometry of Fig. 1(b).<sup>2</sup> Since we are concerned with angular measurements, we will only do the calculation for the geometry of Fig. 1(a). This means that,

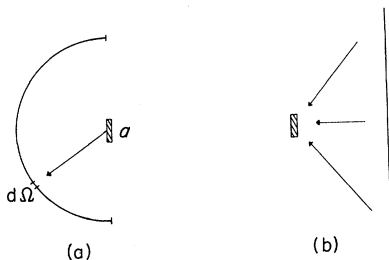


FIG. 1. Schematic view of two possible photoemission experiments. In (a), a sample of area  $\mathcal{A}$  is illuminated with light and gives off electrons which are collected in a hemisphere. An angular measurement would count just those in a unit solid angle  $d\Omega$ . In (b), an infinite surface of sample is illuminated with light, but electrons are collected in an area  $\mathcal{A}$ . These two experiments give the same result for the total yields.

outside the crystal, we must explicitly construct outgoing wave functions in the form

$$\psi(R) = f(\theta, \varphi) e^{iPR}/R,$$

where the amplitude factor  $f(\theta, \varphi)$  determines the amount of photoemission.

Our general model for the surface is shown in Fig. 2. The potential  $V(z)$  is zero for  $z < a$ , and this is the vacuum region. For  $z > b$  we have the solid region, and the in-between region  $a > z > b$  is the surface. Not shown in the figure, but included in the calculations, are the atomic core potentials regularly spaced in the surface and solid region. For a simple metal, we interpret the potential  $V_0$  to be the sum of the Fermi energy  $E_F$  and the work function  $\varphi$ . We assume that the component of wave vector parallel to the surface is conserved at the surface. This is an assumption of specular reflection at the surface. Actually, it is an assumption on the care with which the surface has been prepared for the experiment. Clearly an idealized surface is specular. It is just actual ones, which are irregular, which may not have specular reflection at the surface. Most of the results we obtain would be significantly altered under some other surface condition such as a diffuse reflection. Indeed the angular measurement of photoemission would provide a critical test of surface smoothness and specularity, since a diffuse surface would have no  $\varphi$  dependence in the angular measurement, and certainly no sharp cones of electrons.

New results are, whenever possible, illustrated by numerical examples. The alkali metals have been used in these examples, and Table I shows the parameters we have used in the calculations. But the ideas and conclusions of this paper are not restricted to the alkali metals, but should equally apply to other free-electron metals.

## II. EXTERNAL INTENSITY

In this section we derive an equation for the intensity of external electrons which are measured in photoemission. The physical problem may be stated quite simply: Given that the optical absorption creates a certain distribution of electrons inside the crystal, how many of these electrons actually escape out of the solid? Previous theoretical treatments of this

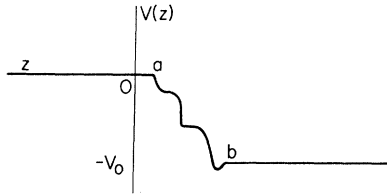


FIG. 2. Schematic representation of the potential shape at the vacuum-solid interface. The vacuum region is  $z < a$ , and the solid region is  $z > b$ . The potential  $-V_0$  is the bottom of the conduction band, so that  $V_0$  equals the Fermi degeneracy plus the work function of the metal.

problem have, at best, added an *ad hoc* transmission coefficient. The main exception is Adawi's calculation of the photoemission of the surface effect, where the external intensity was calculated correctly.<sup>2</sup> There is a clear need for a formalism which rigorously accounts for the transmission properties of the surface, and which can be used for both the volume effect and the surface effect. This will be accomplished in this section.

Let us begin by discussing the simplest possible example. This is a solid which has no band structure whatsoever—it is a free-electron gas. We will also consider just those electrons which leave the solid without suffering any scattering from electron-phonon effects, etc. After this simple case is understood, it is easy to show how to include the effects of many-body interactions and also band structure. First, we need to evaluate the electron Green's function in the presence of the surface

$$G_0(\mathbf{r}, \mathbf{r}', E) = \int d^3\mathbf{k}_{\parallel} \int_0^{\infty} dk_z \sum_i \frac{\psi_i(\mathbf{k}, \mathbf{r}) \psi_i(\mathbf{k}, \mathbf{r}')^*}{E_k - E - i\delta}, \quad (2.1)$$

$$E_k = (k_{\parallel}^2/2m) + E_{k_z}.$$

The wave functions  $\psi_i(\mathbf{k}, \mathbf{r})$  have the following form:

$$\psi_i(\mathbf{k}, \mathbf{r}) = [\exp(i\mathbf{k}_{\parallel} \cdot \rho) / (2\pi)] \phi_i(k_z, z).$$

Consider the surface potential in Fig. 2. For  $k_z$  such that

$$0 > E_{k_z} = (k_z^2/2m) - V_0 > -V_0$$

there is only one wave function  $\phi_1(k_z, z)$  which has the form  $\sin(k_z z - \delta)$  for  $z > b$ . In this case the sum over  $i$  in (2.1) extends only over this one term. But for  $k_z$  such that

$$E_{k_z} = (k_z^2/2m) - V_0 > 0$$

there are two wave functions, and the sum over  $i$  has two terms. The difficult way to obtain the Green's function in (2.1) is to write down all of the wave functions and then to perform the integrals. There is a much easier way. First consider just the  $z$ -com-

ponent of the Green's function

$$G_0(z, z'; \Omega) = \int_0^{\infty} dk_z \sum_i \frac{\phi_i(k_z, z) \phi_i^*(k_z, z')}{E_{k_z} - \Omega - i\delta}, \quad (2.2)$$

$$G_0(\mathbf{r}, \mathbf{r}', E) = \int [d^3\mathbf{k}_{\parallel} / (2\pi)^2] \exp[i\mathbf{k}_{\parallel} \cdot (\boldsymbol{\rho} - \boldsymbol{\rho}')] \times G_0(z, z'; E - k_{\parallel}^2/2m). \quad (2.3)$$

This equation satisfies

$$[-(1/2m)(\partial^2/\partial z^2) + V(z) - \Omega]G_0(z, z'; \Omega) = \delta(z - z'). \quad (2.4)$$

If both  $z$  and  $z'$  are less than  $a$ , and therefore in the region where the potential is zero, then this Green's function must have the form for  $\Omega > 0$

$$G_0(z, z'; \Omega) = (im/p_z) \{ \exp(ip_z |z - z'|) + R \exp[-ip_z(z \pm z')] + R' \exp[ip_z(z \pm z')] \},$$

$$p_z^2 = 2m\Omega.$$

The terms with coefficients  $R$  and  $R'$  satisfy the homogeneous part of (2.4). For photoemission we require that one of these variables, say  $z$ , go to  $-\infty$ , so that  $z < z'$ , in which case the Green's function is

$$G_0(z, z'; \Omega) = (im/p_z) \exp(-ip_z z) [\exp(ip_z z') + R \exp(-ip_z z') + (im/p_z) R' \exp[ip_z(z \pm z')]].$$

We can interpret the term  $\exp(-ip_z z)$  as a plane wave going to the left. Since in the experiment there are no plane-wave electrons coming in from  $-\infty$ , we conclude that the coefficient  $R'$  must be zero. So we can write

$$G_0(z, z'; \Omega) = (im/p_z) \exp(-ip_z z) \phi^{\>}(p_z, z'), \quad (2.5)$$

where for  $z < z' < a$  the ingoing wave function  $\phi^{\>}$  is

$$\phi^{\>}(p_z, z') = \exp(ip_z z') + R \exp(-ip_z z').$$

This has a simple physical interpretation:  $\phi^{\>}$  represents a wave function which has a term  $\exp(ip_z z')$  describing a wave incident upon the crystal from the left, and the term  $R \exp(-ip_z z')$  represents the amount reflected. We conclude immediately that in the region  $z > b$  in Fig. 2 the transmitted wave has the form

$$\phi^{\>} = T \exp(ik_z z').$$

In general, one can determine the form of  $\phi^{\>}$  for all values of  $z$  since it is a solution to Schrodinger's equation

$$\{ -(1/2m)(\partial^2/\partial z^2) + V(z) - \Omega \} \phi^{\>} = 0,$$

with the initial condition of a wave, of unit amplitude, impinging from outside the solid. Thus, as noted by Adawi, in order to obtain the number of electrons which get out of the crystal, one has to calculate the fraction  $T$  which get in. This is not surprising, because the transmission coefficient for getting out of a crystal is proportional to the transmission coeffi-

cient for getting in—the factor of proportionality is just the ratio of velocities inside and out.

Assume that the initial wave function of the electron is  $\phi_i$ , and the applied radiation excites this eigenstate by the  $\mathbf{p} \cdot \mathbf{A}$  interaction

$$\mathcal{H}' = (e/mc) A \hat{\mathbf{e}} \cdot \mathbf{p}. \quad (2.6)$$

Then the wave function of the electron after the optical transition is

$$\psi(\mathbf{R}) = \int d^3r' G_0(\mathbf{R}, \mathbf{r}') \mathcal{H}' \phi_i(\mathbf{r}').$$

For external photoemission, we want  $\mathbf{R} = (\boldsymbol{\rho}, z)$  to be outside of the crystal, and far away, in which case we can use the form of the Green's function derived above:

$$\begin{aligned} \psi(\mathbf{R}) = im \int \frac{d^2p_{||}}{(2\pi)^2} \frac{\exp(-i\mathbf{p}_{||} \cdot \boldsymbol{\rho}) \exp(-ip_z z)}{p_z} \\ \times \int d^3r' \exp(i\mathbf{p}_{||} \cdot \boldsymbol{\rho}') \phi^>(p_z, z') \mathcal{H}' \phi_i(\mathbf{r}'). \end{aligned}$$

The integral over  $d^2p_{||}$  is most easily performed by changing integration variables. In the new variable system, the “ $z$ ” direction is along  $\mathbf{R}$ . Since the length of the vector  $\mathbf{p} = (\mathbf{p}_{||}, p_z)$  is fixed,

$$p^2 = 2m(E_i + \omega), \quad (2.7)$$

the new variables are the angles ( $\nu' = \cos\theta'$ ,  $\varphi'$ ) that  $\mathbf{p}$  makes with respect to  $\mathbf{R}$ . The range of these variables is limited by the requirement  $p_z > 0$ . We get that

$$\begin{aligned} \psi(\mathbf{R}) = \frac{im\hbar}{2\pi^2} \left( \int_{(1-\nu^2)^{1/2}}^1 d\nu' \exp(ipR\nu') \int_0^\pi d\varphi' M(\nu', \varphi') \right. \\ \left. + \int_{-(1-\nu^2)^{1/2}}^{(1-\nu^2)^{1/2}} d\nu' \exp(ipR\nu') \int_0^{\varphi_0} d\varphi' M(\nu', \varphi') \right), \\ M(\nu', \varphi') = \int d^3r' \exp(i\mathbf{p}_{||} \cdot \boldsymbol{\rho}') \phi^>(p_z, z') \mathcal{H}' \phi_i(\mathbf{r}'), \\ \varphi_0 = \cos^{-1}[-\nu\nu' / (1-\nu^2)^{1/2}(1-\nu'^2)^{1/2}], \end{aligned}$$

where  $\nu = \cos\theta$  is the angle that  $\mathbf{R}$  makes with respect to the normal to the surface. Now integrate by parts on the  $d\nu'$  variable, which gives

$$\begin{aligned} \psi(R) = \frac{m}{2\pi^2 R} \left( \exp(ipR) \int_0^\pi d\varphi' M(1, \varphi') \right. \\ \left. - \int_{(1-\nu^2)^{1/2}}^1 d\nu' \exp(ipR\nu') \int_0^\pi d\varphi' \frac{\partial}{\partial \nu'} M(\nu', \varphi') \right. \\ \left. - \int_{-(1-\nu^2)^{1/2}}^{(1-\nu^2)^{1/2}} d\nu' \exp(ipR\nu') \frac{\partial}{\partial \nu'} \int_0^{\varphi_0} d\varphi' M(\nu', \varphi') \right). \end{aligned}$$

The first term goes as  $\exp(ipR)/R$  and is the result we want as  $R \rightarrow \infty$ . The remaining terms fall off as a higher power of  $R$  at large  $R$ . Since at  $\nu' = 1$  the

function  $M(1, \varphi')$  has no  $\varphi'$  dependence, we simply get

$$\lim_{R \rightarrow \infty} \psi(\mathbf{R}) = (m/2\pi R) \exp(ipR) M(\mathbf{p}_{||}, p_z), \quad (2.8)$$

$$M(\mathbf{p}_{||}, p_z) = \int d^3r' \exp(-i\mathbf{p}_{||} \cdot \boldsymbol{\rho}') \phi^>(p_z, z') \mathcal{H}' \phi_i(\mathbf{r}').$$

Of course, in this last expression, the direction of  $\mathbf{p} = (\mathbf{p}_{||}, p_z)$  is now along  $\mathbf{R}$  (since  $\nu' = 1$ ). At large  $R$  the electron current for each initial state is, per unit solid angle  $\delta\Omega$ ,

$$\begin{aligned} R^2 (2e/m) \text{Im} \psi^*(\mathbf{R}) \nabla_R \psi(\mathbf{R}) \\ = (2e/m) (m/2\pi)^2 p |M(\mathbf{p}_{||}, p_z)|^2 [1 + O(1/R)]. \end{aligned}$$

Taking the limit that  $R \rightarrow \infty$ , and summing over initial states, gives the result

$$dI/d\Omega = (2e/m) (m/2\pi)^2 \int [d^3k_i / (2\pi)^3] p |M(\mathbf{p}_{||}, p_z)|^2. \quad (2.9)$$

In evaluating (2.9), keep in mind that the direction of the vector  $\mathbf{p}$  is fixed in the direction  $\mathbf{R}$ , which is just the direction  $(\theta, \varphi)$  at which the angular measurement is being performed. The magnitude of  $p$  does vary with  $k_i$ , as is evident from (2.7).

It is now very simple to include many-body effects in the derivation of the expression for the external current. Assume that one can write the Hamiltonian as

$$\mathcal{H} = \mathcal{H}_0 + V,$$

where  $\mathcal{H}_0$  has as its eigenstates the  $\psi_i(k, r)$  which go into the Green's function (2.1). The interaction  $V$  is the sum of all the perturbations of interest, including the  $\mathbf{p} \cdot \mathbf{A}$  interaction  $\mathcal{H}'$  in (2.6):

$$V = \mathcal{H}' + \mathcal{H}_{\text{el-el}} + \mathcal{H}_{\text{el-phon}} + \mathcal{H}_{\text{el-imp}}.$$

The additional terms represent electron-electron, electron-phonon, and electron-impurity interactions. One may add anything of interest to this list. The multiple scattering by many-body effects is described by a  $T$  matrix

$$\mathcal{H} = V + V G_0 \mathcal{H}.$$

We are only interested in term in  $\mathcal{H}$  where the  $\mathcal{H}'$  interaction acts once, but other interactions may be included as often as desired. After evaluating these terms in the  $T$  matrix, the outgoing electron wave function as  $R \rightarrow \infty$  is simply given by

$$\psi(R) = (m/2\pi R) \exp(ipR) \langle \phi^>* \exp(i\mathbf{p}_{||} \cdot \boldsymbol{\rho}) | \mathcal{H} | \phi_i \rangle.$$

In analogy with (2.9), the current is given by

$$\begin{aligned} dI/d\Omega = (2e/m) (m/2\pi)^2 \\ \times \int [d^3k_i / (2\pi)^3] p |\langle \phi^>* e^{i\mathbf{p}_{||} \cdot \boldsymbol{\rho}} | \mathcal{H} | \phi_i \rangle|^2. \quad (2.10) \end{aligned}$$

If excitations, such as phonons or electron-hole pairs, have been emitted or absorbed, then one must sum over their wave vectors as well. This formula appears to be a useful formula for starting actual many-body

calculations. One can use the "golden rule" technique, which employs the open-diagram method developed by DuBois, Gilinsky, and Kivelson.<sup>10</sup> They have amply demonstrated that this is an efficient way of evaluating high-order scattering effects. It appears much more efficient than the usual closed-loop approach. In this regard, we note that we have not yet been able to derive a simple, time-ordered, correlation function which would serve as the starting point for a closed-loop type of calculation. That is, we have not yet found a "Kubo formula for photoemission." Nor do we accept the recent results of others who have tried to derive one.<sup>5,6,11</sup> Our result (2.10) is perfectly acceptable for an open-diagram calculation.

Next we wish to discuss the modification of (2.9) or (2.10) caused by the band structure of the solid. Our starting point is still the Green's function (2.1), except that now the wave functions  $\psi_i(\mathbf{k}, \mathbf{r})$  are plane waves outside of the crystal and Bloch functions inside. Outside of the solid the Green's function must still have the general form of (2.3) and (2.5). So the problem still reduces to finding the properties of a wave of unit amplitude

$$\exp(i\mathbf{p}_{||}\cdot\boldsymbol{\rho}) \exp(ip_z z) + \text{reflected waves}$$

which is directed at the surface. Of course, this is just the situation in a low-energy electron diffraction (LEED) experiment. In LEED calculations and experiments, one is interested in the property of the reflected waves. In a bulk photoemission experiment, one is interested in the amplitude transmitted into the surface. Otherwise, one can calculate as is done for LEED. For example, following Pendry,<sup>12</sup> if the reciprocal-lattice vectors  $\mathbf{G} = (G_z, \mathbf{G}_{||} = \mathbf{g}_j)$  of the solid have  $\mathbf{g}_j$  as their component parallel to the surface, then the reflected waves will have a  $z$  component given by

$$K_j^2 = 2mE - (\mathbf{p}_{||} + \mathbf{g}_j)^2.$$

The reflected wave will be of the form

$$\sum_j R_j \exp[-iK_j z + i(\mathbf{p}_{||} + \mathbf{g}_j) \cdot \boldsymbol{\rho}].$$

Pendry discusses how to determine the reflected and transmitted wave amplitudes by matching at the surface. Inside the solid, one matches onto the set of Bloch functions  $\Psi(\mathbf{k}_i, \mathbf{r})$

$$\sum_j T_j \Psi(\mathbf{k}_j, \mathbf{r}).$$

Included in the set  $\Psi(\mathbf{k}_i, \mathbf{r})$  are all Bloch functions whose parallel wave vectors  $\mathbf{k}_{i||}$  is equal to  $\mathbf{p}_{||}$  or else  $\mathbf{p}_{||} + \mathbf{g}_j$ . This matching procedure couples to an infinite set of Bloch waves inside, and an infinite set of reflected waves outside. But as in LEED calculations, accurate matching may be obtained by including only a selected finite set of  $\mathbf{g}_j$  values. In our photoemission experiment, the matching to these  $\mathbf{g}_j$  components has a simple physical interpretation. This is discussed in detail in Sec. VII.

The number of electrons which are emitted must be proportional to the flux of photons incident upon the sample. So expressions such as (2.9) and (2.10) must have, as one of the factors on the right-hand side, the photon flux  $F$  (photons/sec)

$$F = (c/n)\mathcal{A}(N_k/V),$$

where  $\mathcal{A}$  is the area of the sample,  $n$  is the refractive index, and  $N_k/V$  is the volume density of photons in the solid. One can also express  $F$  as

$$F = F_0(1-R),$$

where  $F_0$  is the photon flux incident upon the sample in the vacuum, and  $R$  is the reflectivity.

These factors arise from the vector potential

$$A_k = (2\pi\hbar c^2 N_k / n^2 \omega_k V)^{1/2},$$

which is contained in (2.6). Since only terms in the  $T$  matrix  $\mathfrak{J}$  are retained which have  $\mathfrak{J}\mathcal{C}'$  acting once, then (2.10) is proportional to

$$[(e/mc)A_k]^2 = \alpha F (2\pi\hbar^2 / m^2 n \omega_k \mathcal{A}),$$

where  $\alpha = e^2/\hbar c$ .

### III. X-RAY PHOTOEMISSION

The conceptually simplest photoemission experiment has the initial electronic states highly localized. This is the case in x-ray photoemission, and also photoemission from localized valence states. We will derive the distribution of those electrons which start from such states and leave the solid without further scattering. So we will evaluate (2.9). The first step is to select a form for  $\phi^>$  inside the solid. The easiest choice is

$$\phi^>(p_z, z) = T(p_z, k_z) \exp(ik_z z), \quad (3.1)$$

$$k_z^2 = p_z^2 + 2mV_0.$$

The localized state  $\phi_i(\mathbf{r} - \mathbf{R}_j)$  is centered about the lattice site  $\mathbf{R}_j$ . In this case the outgoing electron wave function in (2.8) has the form

$$\psi(R) = (eA/2\pi cR) \exp(ipR) T(p_z, k_z) \hat{\epsilon} \cdot \mathbf{p}_{fi} \exp(i\mathbf{k} \cdot \mathbf{R}_j),$$

$$\mathbf{p}_{fi} = i\hbar \int d^3r \exp(i\mathbf{k} \cdot \mathbf{r}) \nabla \phi_i(\mathbf{r}).$$

Now the sum over initial states involves just a sum over lattice sites

$$dI/d\Omega = (2e/m) (eA/2\pi c)^2 p |T(p_z, k_z)|^2 (\hat{\epsilon} \cdot \mathbf{p}_{fi})^2 \times \sum_j \exp(-2\lambda z_j),$$

where

$$\sum_j \exp(-2\lambda z_j) = n_0 a \mathcal{A} \sum_{z_j > 0} \exp(-2\lambda z_j),$$

where  $n_0$  is the density of localized levels and  $a$  is the spacing between localized levels in the  $z$  direction. The damping factor  $\lambda$  has two possible sources. First, the vector potential (or equivalently, the electric

field) will decay exponentially in the solid as  $\exp(-\kappa\omega z/c)$ , where  $\kappa$  is the extinction coefficient. Second, the electron has a finite mean free path which means that the electron wave vector  $k_z = k_{zR} + ik_{zI}$  is complex. So  $\lambda$  is

$$\lambda = k_{zI} + (\kappa\omega/c), \quad (3.2)$$

$$\sum_{z_j > 0} \exp(-2\lambda z_j) = [1 - \exp(-2\lambda a)]^{-1} \approx (2\lambda a)^{-1}.$$

The last step in the above equation is only valid if  $\lambda a \ll 1$ , but we shall assume this to be the case. The length  $l = \lambda^{-1}$  may be viewed as the thickness of the surface layer which contributes to the photoemission. Collecting all of these factors gives

$$dI/d\Omega = (\epsilon\alpha F \rho l n_0 / 2\pi \hbar^2 \omega n m) |T(p_z, k_z)|^2 (\hat{\epsilon} \cdot \mathbf{p}_{fi})^2. \quad (3.3)$$

This is our basic result for the angular dependence of the photoemission from localized levels. In this model all of the electrons come out at the same energy  $E = E_i + \omega - V_0$ . This is because our simple model neglects the width of the initial state, and also many-body scattering effects. The number of electrons *per energy* per solid angle is simply given by

$$d^2I/d\Omega dE = (dI/d\Omega) \delta(E - E_i - \omega + V_0).$$

The total number of electrons emitted is obtained by integrating (3.3) over all solid angle in the hemisphere:

$$I(\omega) = \int d\Omega \frac{dI}{d\Omega} = \int_0^{2\pi} d\varphi \int_0^1 dv \frac{dI}{d\Omega}.$$

An interesting result is obtained by changing variables to

$$\begin{aligned} \int_0^{2\pi} d\varphi \int_0^1 dv &= \int \frac{d^2 p_{\parallel}}{p p_z} \\ &= \int \frac{d^3 p}{m p} \delta\left(\frac{p^2}{2m} - E_i - \omega + V_0\right) \\ &= \int \frac{d^3 k}{m p} \left(\frac{k_z}{p_z}\right) \delta\left(\frac{k^2}{2m} - E_i - \omega\right). \end{aligned}$$

This gives for the photoemission current

$$\begin{aligned} I(\omega) &= \frac{\epsilon\alpha F n_0 l}{2\pi \hbar^2 \omega m^2 n} \int_{k_z > 0} d^3 k \delta(\epsilon_k - E_i - \omega) \\ &\quad \times [(k_z/p_z) T(p_z, k_z)]^2 (\hat{\epsilon} \cdot \mathbf{p}_{fi})^2. \end{aligned}$$

This result should be compared with the definition of the imaginary part of the dielectric function  $\epsilon_2(\omega) = 2n\kappa$ :

$$\epsilon_2(\omega) = \frac{8\pi^2 e^2 n_0}{m^2 \omega^2} \int_{\text{all } k_z} \frac{d^3 k}{(2\pi)^3} \delta(\epsilon_k - E_i - \omega) (\hat{\epsilon} \cdot \mathbf{p}_{fi})^2.$$

Now if we assume that  $k_z T^2/p_z$  is a constant, or alternatively use a value averaged over the different

angular directions, then the answer is simply

$$I(\omega) = \frac{1}{2} \epsilon F \langle (k_z/p_z) T^2 \rangle_{\text{av}} (1 + k_{zI} c / \omega \kappa)^{-1}.$$

The factors of  $\epsilon_2(\omega)$  cancel in numerator and denominator. This result has a very simple interpretation. The various factors in the expression are  $F$ , the photon flux in the solid, since every photon gets absorbed somewhere and makes one electron energetic enough to get out;  $\frac{1}{2}$ , because of those electrons excited, half are going towards the surface, and half are going away from it.  $(1 + k_{zI} c / \omega \kappa)^{-1}$  is the fraction of those going towards the surface, which actually get to the surface without scattering, and  $\langle k_z T^2 / p_z \rangle$  is the fraction of those, which got to the surface, which do actually get out to the solid. This result has already been anticipated by Baertsch and Richardson.<sup>13</sup> The important point is that the photoemission need not depend significantly on the absorption constant. All of the photons in the solid are usually going to be absorbed somewhere, and it is really more relevant to know how close to the surface this occurs.

#### IV. SURFACE EFFECT

We will adopt the standard model for this calculation.<sup>2</sup> The electrons in the solid are assumed to be a free-electron gas, and the surface is given by a step potential. This model has been considered often in the past, and correct expressions have been derived for the total emission current (yield)  $I(\omega)$ , and the energy distribution  $dI/dE$ . We will calculate the angular dependence of these two quantities.

Our calculation can proceed directly from (2.9). In order to simplify the evaluation of the matrix element, we replace the operator  $\hat{\epsilon} \cdot \nabla$  by the equivalent result

$$\begin{aligned} \langle \phi \rangle^* \exp(i\mathbf{p}_{\parallel} \cdot \boldsymbol{\rho}) | \hat{\epsilon} \cdot \nabla | \phi_i \rangle &= [i(\hat{\epsilon} \cdot \hat{z}) / \hbar \omega] \\ &\quad \times \langle \phi \rangle^* \exp(i\mathbf{p}_{\parallel} \cdot \boldsymbol{\rho}) | (\partial/\partial z) V(z) | \phi_i \rangle, \end{aligned}$$

where  $V(z)$  is the potential at the surface. Wave vector is conserved parallel to the surface  $\mathbf{k}_{i\parallel} = \mathbf{k}_{\parallel} = \mathbf{p}_{\parallel}$ :

$$M = a \delta_{\mathbf{k}_{i\parallel}, \mathbf{p}_{\parallel}} [( \hat{\epsilon} \cdot \hat{z} ) / \hbar \omega] (eA/mc) \langle \phi \rangle^* | \partial V / \partial z | \phi_i(z) \rangle,$$

so that

$$\begin{aligned} dI/d\Omega &= [\epsilon\alpha F (\hat{\epsilon} \cdot \hat{z})^2 / 2\pi^2 m \omega^3 n] \\ &\quad \times \int d^3 \mathbf{k}_i \delta(\mathbf{k}_{i\parallel} - \mathbf{p}_{\parallel}) p | \langle \phi \rangle^* | \partial V / \partial z | \phi_i \rangle|^2. \end{aligned}$$

The  $\delta$  function eliminates the integration over  $d^2 \mathbf{k}_{i\perp}$ , but this step is slightly tricky, since  $\mathbf{p}_{\parallel}$  depends upon  $\mathbf{k}_{\parallel}$ ; this arises because

$$p_{\parallel} = \sin\theta [k_i^2 + 2m(\omega - V_0)]^{1/2},$$

where  $\theta$  is the angle at which the external current is being measured:

$$\int d^2 \mathbf{k}_{i\perp} \delta(\mathbf{k}_{i\perp} - \mathbf{p}_{\perp}) = \cos^{-2}\theta$$

and

$$p = [k_{iz}^2 + 2m(\omega - V_0)]^{1/2} / \cos\theta.$$

This gives for the angular dependence of the yield

$$dI/d\Omega = [e\alpha F(\hat{\epsilon} \cdot \hat{z})^2 / 2\pi^2 m \omega^3 n] \int dk_{iz} (p/\cos^2\theta) \times |\langle \phi^{>*} | \partial V/\partial z | \phi_i \rangle|^2. \quad (4.1)$$

This last integration can only be performed after  $\partial V/\partial z$  is determined from the properties of the surface. For a step potential,

$$\begin{aligned} \partial V/\partial z &= -V_0 \delta(z), \\ \langle \phi^{>*} | \partial V/\partial z | \phi_i \rangle &= -V_0 \phi^{>}(0) \phi_i(0) \\ &= (-2p_z k_{iz}/m) [(k_z - p_z)/(k_z + p_z)]^{1/2}. \end{aligned} \quad (4.2)$$

If (4.2) is inserted into (4.1), the integral over  $dk_{iz}$  may be evaluated in an analytical fashion. This result, which is somewhat lengthy, is given in the Appendix.

The total current  $I(\omega)$  is obtained by integrating over the external solid angle:

$$I(\omega) = \int d\Omega (dI/d\Omega). \quad (4.3)$$

If we put (4.1) into the above expression, and shuffle variables of integration, we obtain exactly the result for  $I(\omega)$  previously derived by Adawi. For the step potential, the integrals may be done analytically, and these results are also given in the Appendix.

The current per solid angle per energy  $d^2I/d\Omega dE$  is defined as

$$dI/d\Omega = \int dE (d^2I/dE d\Omega).$$

This may be derived from (4.1) by inserting a delta function for energy conservation under the integral. The energy must be expressed in terms of the independent variables, which, in (4.1), give the result

$$\begin{aligned} \frac{d^2I}{dE d\Omega} &= \frac{e\alpha F(\hat{\epsilon} \cdot \hat{z})^2}{2\pi^2 m \omega^3 n} \int_0^{k_F} dk_{iz} \frac{p}{\cos^2\theta} \left| \langle \phi^{>*} | \frac{\partial V}{\partial z} | \phi_i \rangle \right|^2 \\ &\quad \times \delta\left(E - \frac{k_{iz}^2/2m + \omega - V_0}{\cos^2\theta}\right). \end{aligned}$$

The integral over  $dk_{iz}$  may be performed immediately, and

$$\begin{aligned} \frac{d^2I}{d\Omega dE} &= \frac{e\alpha F(\hat{\epsilon} \cdot \hat{z})^2}{2\pi^2 (\hbar\omega)^3 n} \frac{E^{1/2}}{(E \cos^2\theta + V_0 - \omega)^{1/2}} \\ &\quad \times |\langle \phi^{>*} | \partial V/\partial z | \phi_i \rangle|^2. \end{aligned} \quad (4.4)$$

For the step potential, the matrix element (4.2) has the form in (4.4)

$$\begin{aligned} |\langle \phi^{>*} | \partial V/\partial z | \phi_i \rangle|^2 &= 16 \cos^2\theta (E/V_0) (E \cos^2\theta + V_0 - \omega) \\ &\quad \times [(E \cos^2\theta + V_0)^{1/2} - E^{1/2} \cos\theta]^2. \end{aligned} \quad (4.5)$$

At low photon energies photoemission is believed to come largely from the surface effect. So a measurement of  $d^2I/d\Omega dE$  at low photon energies provide a means of measuring the square of the matrix element  $|\langle \phi^{>*} | \partial V/\partial z | \phi_i \rangle|^2$ . Also note that the surface effect has a characteristic polarization dependence  $(\hat{\epsilon} \cdot \hat{z})^2$

which appears unique among the mechanisms contributing to the external current of electrons, so one should be able to measure which fraction of the photoemission current came from the surface effect by determining which fraction of the current had this dependence. The volume contribution to photoemission, which will be discussed in Sec. V, has a polarization dependence  $(\hat{\epsilon} \cdot \mathbf{G})^2$ . So if the sample is aligned such that none of the important reciprocal-lattice vectors  $\mathbf{G}$  are in the  $z$  direction, then only the surface effect will have the dependence  $(\hat{\epsilon} \cdot \hat{z})^2$ . This discussion assumes a specularly smooth surface. For a rough surface, there will probably be absorption by the surface effect even for polarizations not in the  $z$  direction.

The energy distribution curves  $dI/dE$  are obtained from (4.4) by integrating over the external angular variables

$$dI/dE = \int d\Omega (d^2I/d\Omega dE). \quad (4.6)$$

This integral is the same as obtained previously by Adawi. It may be evaluated analytically, and the result is also given in the Appendix.

## V. VOLUME EFFECT

We begin the discussion of the volume effect by discussing the properties of the alkali metals. We assume that they are a nearly-free-electron metal. By this we mean that band-structure effects will be included insofar as they cause optical absorption, but not their effect on distorting the energy bands. A more complete discussion, with the band distortions included, will also be given below. But first we wish to stress some simple ideas which are most clearly presented for a free-electron gas. As will be shown later, band distortions have little effect upon these simple results.

In a nearly-free-electron gas, optical absorption may be viewed as a two-step process. The absorption of the photon provides the electron with the additional energy it needs to get to the excited state. The crystal potential imparts to the electron the additional momentum it needs to reach the excited state. This momentum comes in multiples of the reciprocal-lattice vectors  $\mathbf{G}$ . So in a reduced-zone picture, the transitions are vertical in wave-vector space. But in photoemission, it is more useful to think in an extended-zone scheme.

First consider what happens inside of the solid, during the ordinary interband absorption. Let  $\mathbf{K}$  be the final wave vector of the electron, and  $\mathbf{K}-\mathbf{G}$  the initial wave vector. In an alkali metal,  $\mathbf{K}-\mathbf{G}$  is within the first Brillouin Zone, and  $\mathbf{K}$  is outside of it. Energy conservation requires

$$K^2/2m = (\mathbf{K}-\mathbf{G})^2/2m + \omega.$$

Solving this equation for  $K$ , we get, with  $E_G = G^2/2m$ ,

$$(KG \cos\theta_0)/m = \omega + E_G \equiv \Lambda,$$

where  $\theta_0$  is the angle between  $\mathbf{K}$  and  $\mathbf{G}$ . Thus

$$E = K^2/2m = \Lambda^2/4E_G \cos^2\theta_0. \quad (5.1)$$

This simple-looking equation contains most of the physics of the angular dependence of photoemission for a free-electron metal. To appreciate this equation, think spatially. An electron whose final-state wave vector  $\mathbf{K}$  makes an angle  $\theta_0$  with  $\mathbf{G}$  has an energy given by (5.1). Alternately, all electrons have the same energy which have the same angle  $\theta_0$  with respect to  $\mathbf{G}$ . So electrons with the same energy form a conical distribution, where  $\mathbf{G}$  is the center of the cone. Those electrons with a larger cone angle  $\theta_0$  have a larger energy. Furthermore, as will be shown later, the intensity per unit solid angle of this internal distribution goes as

$$dI/d\Omega \sim E/\cos\theta_0 \sim 1/\cos^3\theta_0.$$

So the intensity of electrons increases as the cone angle increases. Therefore, in these cones of electrons, both the energy and intensity increase as the cone angle gets larger. The intensity of these cones increases up to an angle  $\theta_{\max}$ , at which the intensity drops discontinuously to zero. The maximum initial energy an electron may have is  $E_F$ , so the maximum final energy is

$$E < E_F + \omega.$$

If we use (5.1) for  $E$  in this inequality, then

$$1 \geq \cos^2\theta_0 \geq \Lambda^2/4E_G(E_F + \omega) \quad (5.2)$$

and the maximum cone angle is given by

$$\theta_{\max} = \cos^{-1}[\Lambda/2(E_F + \omega)^{1/2}E_G^{1/2}].$$

The inequality (5.2) is quite familiar. If we take its outer parts, then the statement that

$$1 \geq \Lambda^2/4E_G(E_F + \omega)$$

is well known for optical absorption in the alkali metals. It provides the limits on  $\omega$  over which the absorption exists:

$$\omega_{20} = 2(E_G E_F)^{1/2} + E_G \geq \omega \geq E_G - 2(E_G E_F)^{1/2} = \omega_{10}. \quad (5.3)$$

$\theta_{\max}$  has the value of zero at the lower and upper limit of absorption frequencies. For  $\omega$  values between these limits,  $\theta_{\max}$  rises to some maximum value and decreases again to zero. For  $\mathbf{G} = 2\pi(1, 1, 0)/a$  lattice vectors in the alkali metals,  $\theta_{\max}$  has a maximum value of  $26^\circ$  at  $\omega \simeq 0.6E_G$ . Since nearby (110) lattice vectors are  $60^\circ$  apart, this means that the cones of electrons centered on these reciprocal-lattice vectors never overlap.

The angular distribution of electrons in external photoemission is determined by projecting these cones outwards through the surface of the solid. We assume that the orientation of the crystal, with regard to the surface, is known. The reciprocal-lattice vector  $\mathbf{G}$  has components parallel  $\mathbf{G}_{||}$  and normal  $G_z$  to the surface.

In the interband optical transition, let  $\mathbf{K}-\mathbf{G}$  be the initial wave vector of the electron and  $\mathbf{K}$  be the final wave vector inside the solid. The wave vector  $\mathbf{K} = (k_{||}, k_z)$  has components parallel and normal to the surface. Let  $\mathbf{p} = (p_{||}, p_z)$  be the electrons wave vector outside the solid. Clearly, the final energy outside, relative to the vacuum level, is

$$E = p^2/2m.$$

Since we assume specular boundary conditions at the surface, then  $k_{||} = p_{||}$ . Furthermore, the final energy of the electron inside the crystal is

$$E = K^2/2m - V_0,$$

from which we deduce that

$$k_z^2 = p_z^2 + 2mV_0.$$

Lastly, the final energy is the initial energy plus  $\omega$ , so that

$$\begin{aligned} E &= (\mathbf{K}-\mathbf{G})^2/2m - V_0 + \omega \\ &= (K^2/2m) - V_0 + \Lambda - (1/m)(k_z G_z + \mathbf{k}_{||} \cdot \mathbf{G}_{||}). \end{aligned}$$

The first two terms on the right-hand side equal  $E$  and hence cancel the left-hand side. If we relate  $k_z$  and  $k_{||}$  to  $E$ , and let  $\varphi$  be the angle between  $\mathbf{p}_{||}$  and  $\mathbf{G}_{||}$ , then the remaining terms reduce to

$$\frac{1}{2}\Lambda = E_z^{1/2}[E \cos^2\theta + V_0]^{1/2} + (EE_{||})^{1/2} \sin\theta \cos\varphi, \quad (5.4)$$

where  $E_z = G_z^2/2m$  and  $E_{||} = G_{||}^2/2m$ . This result relates the external angles ( $\theta, \varphi$ ) to the other parameters  $E, \omega, G$ , and  $V_0$ . One can solve it a variety of ways. The energy  $E$  may be obtained as a function of  $\theta$  and  $\varphi$ :

$$\begin{aligned} E = \epsilon(\theta, \varphi) &= (\Lambda/2D)^2 \{ E_z^{1/2} (\cos^2\theta - 4V_0 D/\Lambda^2)^{1/2} \\ &\quad - E_{||}^{1/2} \sin\theta \cos\varphi \}^2, \quad (5.5) \end{aligned}$$

$$D = E_z \cos^2\theta - E_{||} \sin^2\theta \cos^2\varphi.$$

Alternatively, for a fixed value of  $E$  one may use (5.4) to relate the angles  $\theta$  and  $\varphi$ . For example,

$$\begin{aligned} \sin\theta &= \frac{\Lambda}{2dE^{1/2}} \left[ E_{||}^{1/2} \cos\varphi \pm E_z^{1/2} \left( \frac{4d(E+V_0)}{\Lambda^2} - 1 \right)^{1/2} \right], \\ d &= E_{||} \cos^2\varphi + E_z. \quad (5.6) \end{aligned}$$

This latter form is quite useful for plotting contours of constant energy for the external photoemission. It has a simple form in the case that  $\varphi=0$ . If  $\theta_G$  is the angle  $\mathbf{G}$  makes with  $z$ , and  $\theta_0$  is the angle  $\mathbf{K}$  makes with  $\mathbf{G}$ , then for  $\varphi=0$

$$\sin\theta = [(E+V_0)/E]^{1/2} \sin(\theta_G \pm \theta_0).$$

Table II shows some values of  $\theta_0$  and  $\theta$  for the case  $\varphi=0$ ,  $\theta_G=45^\circ$ , and  $\hbar\omega=5.0$  eV.

Some examples of these contours are given in Fig. 3. This figure shows some calculations of contours of



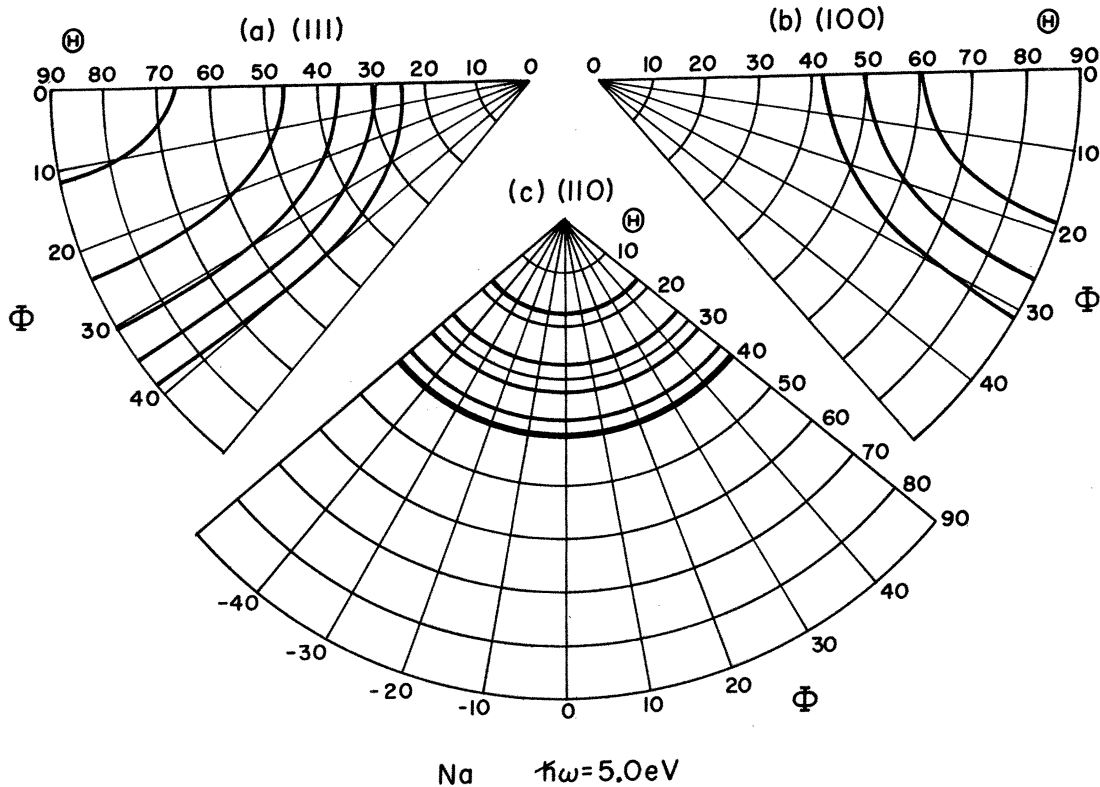


FIG. 3. Angular distribution of the primary cones of external electrons for Na at  $\hbar\omega = 5.0$  eV. The solid lines are contours of constant energy. The outer line is  $E_{\max} = 2.75$  eV and is the edge of the cone, while successive lines are lower in energy by increments of 0.25 eV. The three cases (a)–(c) represent the three crystal faces: (a) has  $E_z = \frac{2}{3}E_G$ ,  $E_{\parallel} = \frac{1}{3}E_G$ , (b) has  $E_z = E_{\parallel} = \frac{1}{2}E_G$ , and (c) has  $E_z = E_G$ ,  $E_{\parallel} = 0$ .

constant energy for Na with  $\hbar\omega = 5.0$  eV. One can see that the conical shape is distorted outside the crystal—the distortion arises from the refractive properties of the surface. The data used in computing these curves are shown in Tables I–III. Table III summarizes the orientation of the reciprocal-lattice vectors  $2\pi(110)/a$  with the three main crystal faces. The important parameter is how the energy  $E_G$  is divided between normal  $E_z$  and parallel  $E_{\parallel}$  components. External photoemission is only carried by  $\mathbf{G}$ 's which stick out of the surface. Photoemission may not occur even if the  $\mathbf{G}$  sticks out of the plane. For example, the lattice vectors with  $E_z = \frac{1}{4}E_G$  in the (110) face do not lead

TABLE II. Some angular values (in deg) at  $\hbar\omega = 5.0$  eV.  $\theta_0$  is the maximum internal cone angle, while  $\theta$  is the angle of the external cone edge at  $\varphi = 0$ .  $\delta$  and  $\delta'$  are the changes in these quantities in the two-band model. These results are for a (100) face.

Metal	$\theta_0$	$\theta$	$\delta'$	$\delta$
Na	22	43	-1.1	2.7
K	24	35	-1.3	2.6

to direct photoemission in the case shown in Fig. 3(b). Figure 3 shows the angular distribution of photoemission about one of the main  $\mathbf{G}$ 's in each of the three faces (111), (100), and (110). Only half a distribution is shown in Figs. 3(a) and 3(b) because the

TABLE III. Principal lattice vectors which project out of the three crystal faces of the alkali metals.  $E_z$  and  $E_{\parallel}$  are the components of  $E_G$  which are normal and parallel to the surface.

Crystal face	$\mathbf{G}(a/2\pi)$	$E_{\parallel}/E_G$	$E_z/E_G$
(001)	$(1, 0, 1) (\bar{1}, 0, 1)$	$\frac{1}{2}$	$\frac{1}{2}$
	$(0, 1, 1) (0, \bar{1}, 1)$		
(011)	$(0, 1, 1)$	0	1
	$(1, 0, 1) (\bar{1}, 0, 1)$		
	$(1, 1, 0) (\bar{1}, 1, 0)$		
(111)	$(1, 0, 1) (0, 1, 1)$	$\frac{1}{3}$	$\frac{2}{3}$
	$(1, 1, 0)$		

result is symmetric about  $\varphi=0$ . The energy contour lines are stepped down in units of 0.25 eV, beginning with the maximum energy of  $E_{\max}=2.75$  eV. So in case (b) the three contour lines are 2.75, 2.50, and 2.25 eV. The absence of any other lines means that all electrons are emitted in the range  $2.00 < E \leq 2.75$  eV.  $E_{\max}$  is always the outer contour line, since it defines the maximum cone angle and the intensity discontinuity at the outer limits of the cone.

The (110) face is interesting because  $\mathbf{G}$  is exactly normal to the surface. So the contours of constant energy, which inside of the crystal are circles, are also circles outside. Figure 3(c) only shows part of these circles. The case with  $\mathbf{G}$  normal to the surface has an interesting characteristic. From the two relations

$$E = K^2/2m = \Lambda^2/4E_G \cos^2\theta_0,$$

$$k_z = K \cos\theta_0 = \Lambda(m/2E_G)^{1/2},$$

we see that  $k_z$  is independent of  $\theta_0$ . All electrons in the cone have the same value of  $k_z$ . But since  $p_z = (k_z^2 - 2mV_0)^{1/2}$ , they also all have the same value of  $p_z$ . In surface models with specular matching, the transmission coefficient  $T(p_z, k_z)$  depends only upon  $p_z$  and  $k_z$ , and is therefore the same for all electrons in the cone.

These cones of electrons will be called the *primary* cones, and the name is applied to the shape of the cones both inside and outside of the solid. We shall see below that the crystal potential causes cones to appear in other directions. These other cones are much weaker in intensity, and shall be called *secondary* cones. The primary cones are those which, inside of the solid, have their center along the direction of the reciprocal-lattice vector.

Now we wish to calculate the angular intensity of the electrons outside of the solid. The first step is to determine the initial wave functions  $\phi_i$ . Since the electrons in this state are confined to the solid, the wave functions must be a standing wave of the form

$$\phi_i(\mathbf{k}_i, \mathbf{r}) = \exp(i\mathbf{k}_{i||} \cdot \boldsymbol{\rho}) \{ \exp[i(k_{iz}z - \delta)] - \exp[-i(k_{iz}z - \delta)] \}. \quad (5.7)$$

The wave-vector dependence of the phase shift  $\delta(k)$  depends upon the shape of the surface potential. We will not need to know this detail for our discussion.

The crystal potential is assumed to be a sum of screened local potentials, which are centered at each atom site:

$$V(\mathbf{r}) = \sum_{z_j > 0} v(\mathbf{r} - \mathbf{R}_j).$$

The screened local potential has a Fourier transform

$$V(q) = (1/\Omega_0) \int d^3\mathbf{r} v(\mathbf{r}) \exp(i\mathbf{q} \cdot \mathbf{r}), \quad (5.8)$$

where  $\Omega_0$  is the volume of the unit cell of the solid. Again we employ the step-saving device of replacing the matrix element of  $\mathbf{p} \cdot \mathbf{A}$  by the equivalent ex-

pression

$$\langle \phi^* \exp(i\mathbf{k}_{i||} \cdot \boldsymbol{\rho}) | \hat{\boldsymbol{\epsilon}} \cdot \nabla | \phi_i \rangle = (i/\hbar\omega) \langle | \hat{\boldsymbol{\epsilon}} \cdot \nabla V(\mathbf{r}) | \rangle. \quad (5.9)$$

Inside the solid the ingoing wave  $\phi^>$  has the transmitted form

$$\phi^>(p_z, z) = T(p_z, k_z) \exp(ik_z z) \exp(i\mathbf{k}_{i||} \cdot \boldsymbol{\rho}).$$

So we may write for our matrix element (5.9)

$$\begin{aligned} \langle \phi^* \exp(-i\mathbf{k}_{i||} \cdot \boldsymbol{\rho}) | \hat{\boldsymbol{\epsilon}} \cdot \nabla | \phi_i \rangle &= T(p_z, k_z) \sum_j \int d^3\mathbf{r} \exp(ik \cdot \mathbf{r}) \hat{\boldsymbol{\epsilon}} \cdot \nabla v(\mathbf{r} - \mathbf{R}_j) \phi_i \\ &= i\Omega_0 T(p_z, k_z) \sum_j \exp[i\boldsymbol{\rho}_j \cdot (\mathbf{k}_{i||} + \mathbf{k}_{i||})] \\ &\quad \times \{ \exp[i(k_z + k_{zj}z_j - \delta)] \hat{\boldsymbol{\epsilon}} \cdot [\mathbf{k}_{i||} + \mathbf{k}_{i||} + \hat{\boldsymbol{z}}(k_z + k_{iz})] \\ &\quad \times V[\mathbf{k}_{i||} + \mathbf{k}_{i||} + \hat{\boldsymbol{z}}(k_z + k_{iz})] \\ &\quad - \text{same}(k_{iz} \rightarrow -k_{iz}, \delta \rightarrow -\delta) \}. \end{aligned}$$

The sum over  $\mathbf{R}_j$  sites parallel to the surface requires conservation of parallel wave vector

$$\sum_{\boldsymbol{\rho}_j} \exp[i\boldsymbol{\rho}_j \cdot (\mathbf{k}_{i||} + \mathbf{k}_{i||})] = (\mathcal{A}/\mathcal{A}_0) \sum_{\mathbf{G}_{i||}} \delta_{\mathbf{k}_{i||} + \mathbf{k}_{i||} - \mathbf{G}_{i||}},$$

where  $\mathcal{A}$  is the area of the sample and  $\mathcal{A}_0$  is the area of a unit cell. One is left with the sum over  $z_j$ . This cannot cause wave-vector conservation in the  $z$  direction because the sum only extends over the half-space  $z_j > 0$ . We shall soon see that one still gets an effective wave-vector conservation in this direction anyway. If  $a$  is the lattice constant in the  $z$  direction  $\Omega_0 = a\mathcal{A}_0$ , then the sum over  $z_j$  may be performed to give

$$\sum_{z_j} \exp[iz_j(k_z + k_{zi})] = \{1 - \exp[ia(k_z + k_{zi})]\}^{-1}$$

and

$$\begin{aligned} \langle \phi^* \exp(i\mathbf{k}_{i||} \cdot \boldsymbol{\rho}) | \hat{\boldsymbol{\epsilon}} \cdot \nabla | \phi_i \rangle &= ia\mathcal{A}T \sum_{\mathbf{G}_{i||}} \delta_{\mathbf{k}_{i||} + \mathbf{k}_{i||} - \mathbf{G}_{i||}} \\ &\quad \times \{ e^{-i\delta} \hat{\boldsymbol{\epsilon}} \cdot [\mathbf{G}_{i||} + \hat{\boldsymbol{z}}(k_z + k_{zi})] V[\mathbf{G}_{i||} + \hat{\boldsymbol{z}}(k_z + k_{zi})] \\ &\quad - \text{same}(k_{zi} \rightarrow -k_{zi}, \delta \rightarrow -\delta) \}. \quad (5.10) \end{aligned}$$

Now the angular current in (2.9) is dependent upon the square of this matrix element. The squaring process actually simplified the expression. First consider the factors

$$[\mathcal{A} \sum_{\mathbf{G}_{i||}} \delta_{\mathbf{k}_{i||} + \mathbf{k}_{i||} - \mathbf{G}_{i||}}]^2 = \mathcal{A} (2\pi)^2 \sum_{\mathbf{G}_{i||}} \delta(\mathbf{k}_{i||} + \mathbf{k}_{i||} - \mathbf{G}_{i||}).$$

Next consider the factor

$$\begin{aligned} |1 - \exp[ia(k_z + k_{zi})]|^{-2} \\ = [(1 - e^{-\lambda a})^2 + 4e^{-\lambda a} \sin^2 \frac{1}{2}(k_z + k_{zi})a]^{-1}. \end{aligned}$$

The damping factor  $\lambda$  has been introduced. It has two sources. First, the electron wave vector  $k_z$  may be complex. Second, the photon field may decay into the solid at the surface

$$A(\mathbf{r}) = A \exp(-\kappa\omega z/c),$$

where  $\kappa$  is the extinction coefficient. So we take  $\lambda$  to be the combination of these effects

$$l^{-1} = \lambda = k_{zI} + \kappa\omega/c. \quad (5.11)$$

If  $\lambda a \ll 1$  then one can write

$$|1 - \exp[i(k_z + k_{iz})a]|^{-2} \cong (\pi l/a) \sum_{G_z} \delta(k_z + k_{iz} - G_z).$$

The distance  $l = \lambda^{-1}$  is the effective surface depth which contributes to the photoemission process. It may be determined by the depth of penetration of the incident electric field, or else by the electron mean free path, or a combination of both. Since usually  $\kappa\omega a/c \ll 1$ , the requirement that  $\lambda a \ll 1$  merely means that the electron mean free path is large compared to a lattice dimension. This must be true in order that the wave vector of the electron be well enough defined that one can talk about "wave-vector conservation." Of course, if  $\lambda a \gtrsim 1$  then the photoemitted electrons all emanate from the surface, and it is ridiculous to talk about a bulk photoemission process anyway.

In (5.10) the square of the second term is the same as the square of the first except that  $k_{iz}$  is replaced by  $-k_{iz}$ . In the final integral over  $k_i$  in (2.9), the  $k_{iz}$  values are limited to the space  $k_{iz} > 0$ , since this is appropriate for initial wave functions of the form (5.7). But the two terms of  $k_{iz}$  and  $-k_{iz}$  may be combined into one term with limits of integration  $-\infty, \infty$ . Considering these terms in (2.9) gives the result for the angular intensity

$$dI/d\Omega = [e\alpha Fl/\pi(\hbar\omega)^3 n] \sum_G [(\hat{\epsilon} \cdot \mathbf{G})^2/G] V_G^2 J_G(\theta, \varphi), \quad (5.12)$$

$$J_G(\theta, \varphi) = (G/2m) \int d^3\mathbf{k}_i \delta(\mathbf{K} - \mathbf{k}_i - \mathbf{G}) p |T(p_z, k_z)|^2. \quad (5.13)$$

We still need to examine the cross terms which arise when we square the two terms in (5.10). In the limit that  $\lambda a \ll 1$ , these cross terms also give approximate wave-vector conservation in the  $z$  direction, but the coefficient of the term is smaller by a factor of  $\lambda a$  than (5.12). So we shall assume  $\lambda a \ll 1$  and thereby neglect this term. Of course, it should be included if  $\lambda a \gtrsim 1$ , but then photoemission is a surface effect.

The result (5.12) has the appearance of a simple theory which directly assumed wave-vector conservation. That is, if we started from our original matrix element and just assumed bulk wave-vector conservation

$$\begin{aligned} \langle \phi^* \exp(i\mathbf{k}_{||} \cdot \boldsymbol{\rho}) | \hat{\epsilon} \cdot \nabla V | \phi_i \rangle \\ = \mathcal{V} T(p_z, k_z) \sum_G (\hat{\epsilon} \cdot \mathbf{G}) V_G \delta_{\mathbf{K} - \mathbf{k}_i - \mathbf{G}}, \end{aligned}$$

then we would get a result very similar to (5.12). In fact, the result is identical to (5.12) except a factor of 2 larger.

The integral in (5.13) may be evaluated by noticing that the delta function eliminates the integration. This step is more deceptive than it first appears because  $\mathbf{K}$  is a function of  $\mathbf{k}_i$ . This occurs because the energy is  $E = k_i^2/2m + \omega - V_0$ ; recall that

$$\begin{aligned} k_{||} = p_{||} = (2mE)^{1/2} \sin\theta, \\ k_z = (p_z^2 + 2mV_0)^{1/2} = (2m)^{1/2} (E \cos^2\theta + V_0)^{1/2}. \end{aligned} \quad (5.14)$$

Not only the magnitude, but also the direction of  $\mathbf{K}$  depends upon  $\mathbf{k}_i$ . This is in contrast to the vector  $\mathbf{p}$ , whose direction  $(\theta, \varphi)$  is fixed in the direction of the experiment. Evaluating (5.13) gives

$$\begin{aligned} J_G(\theta, \varphi) = \epsilon(\theta, \varphi) |T(p_z, k_z)|^2 / \cos\theta', \\ \cos\theta' = [(p_z/k_z) \cos\theta G_z + \sin\theta \cos\varphi G_{||}] / G^{-1}. \end{aligned} \quad (5.15)$$

In this expression,  $k_z$  and  $p_z$  still have the meaning given in (5.14), but now  $E$  has the meaning of (5.5).

The total external photoemission yield is obtained by integrating the above result over solid angle:

$$I(\omega) = \int d\Omega (dI/d\Omega).$$

The energy distribution curves, or current per unit energy, are obtained by inserting a  $\delta$  function for energy conservation in the integral for the yield:

$$dI/dE = \int d\Omega (dI/d\Omega) \delta(E - \epsilon(\theta, \varphi)). \quad (5.16)$$

For a step potential at the surface, this integral for  $dI/dE$  may be performed analytically. This lengthy result is given in the Appendix.

One aspect of the result for  $dI/dE$  deserves comment. *Inside* the solid, the distribution  $dI/dE$  is a constant, independent of energy,

$$\begin{aligned} (dI/dE)_{\text{int}} = [e\alpha Fl/(\hbar\omega)^3] \sum_G [(\hat{\epsilon} \cdot \mathbf{G})^2/G] V_G^2 \\ \text{if } E_F + \omega \geq E \geq \Lambda^2/4E_G \\ = 0 \quad \text{otherwise.} \end{aligned}$$

This can be proved quite simply by noting that

$$J_G(\theta, \varphi)_{\text{int}} = \Lambda^2/4E_G \cos^3\theta_0 = \frac{1}{2} (d\epsilon_{\text{int}}/d\theta_0) (\sin\theta_0)^{-1},$$

so that

$$\int d\Omega J_G(\theta, \varphi)_{\text{int}} \delta(E - \epsilon(\theta, \varphi)_{\text{int}}) = \pi.$$

Figure 4 shows some calculated values of  $dI/dE$  for the three crystal faces of Na at  $\hbar\omega = 5.0$  eV. Actually, what is plotted in Fig. 4 is the dimensionless quantity  $K_G(E)$ , which is defined as

$$K_G(E) = \int d\Omega J_G(\theta, \varphi) \delta(E - \epsilon(\theta, \varphi)), \quad (5.17)$$

$$dI/dE = [e\alpha Fl/\pi(\hbar\omega)^3 n] \sum_G [(\hat{\epsilon} \cdot \mathbf{G})^2/G] V_G^2 K_G(E),$$

which is evaluated in the Appendix. Figure 4 is closely correlated with Fig. 3. For example, the range of allowed  $E$  value correlates with the number of energy contour lines in Fig. 3. The crystal face (110) has

a step function distribution for  $K_G(E)$  because that is the distribution inside of the crystal, and we already noted that  $T(p_z, k_z)$  is independent of  $E$  for the special case of  $\mathbf{G}$  normal to the surface. Indeed, for  $\mathbf{G} \parallel \hat{z}$  we get

$$K_G(E) = \pi(k_z/p_z) |T(p_z, k_z)|^2 \quad \text{if } E_{\max} > E > \Lambda^2/4E_G - V_0. \quad (5.18)$$

The result for  $\mathbf{G}$  not normal is much more complicated, as is shown in the Appendix. For the (100) and (111) faces, the external EDC is more of a sawtooth shape, and has no resemblance to the internal values of  $dI/dE$ . We note that the experimental values of  $dI/dE$  for the unscattered electrons have a sawtooth shape.<sup>14,15</sup> It is not possible to give a comparison between theory and experiment because the experimental crystal orientations were not known. We just remark that the shape of the EDC does depend upon crystal orientation, and in some cases has the sawtooth shape observed experimentally.

The last subject we wish to discuss in this section is the possible interference between the surface-effect and the volume-effect mechanisms for photoemission. The total matrix element between the initial and final state is

$$\langle \phi \rangle^* \exp(i\mathbf{k}_{||} \cdot \boldsymbol{\rho}) | \hat{\epsilon} \cdot \nabla V(v) | \phi_i \rangle \\ = \hat{\epsilon} \cdot \hat{z} \langle V_0 \delta(z) | \rangle + \sum_{\mathbf{G}} i \hat{\epsilon} \cdot \mathbf{G} V_G \langle \exp(i\mathbf{G} \cdot \mathbf{r}) | \rangle.$$

When this total expression is squared and put into (2.9), then the two terms in the above expression will have cross products

$$(\hat{\epsilon} \cdot \hat{z}) \langle V_0 \delta(z) | \rangle (\hat{\epsilon} \cdot \mathbf{G}) V_G \langle \exp(i\mathbf{G} \cdot \mathbf{r}) | \rangle,$$

which are interference between the volume and sur-

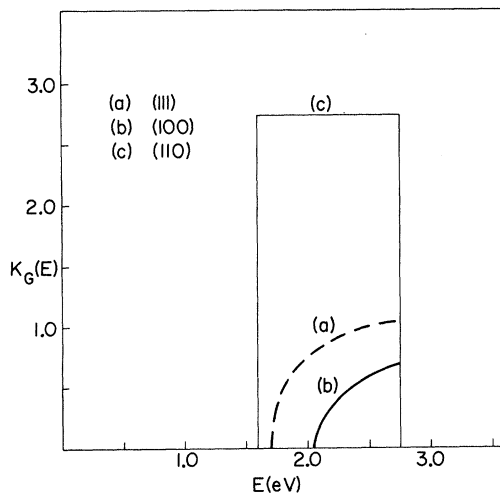


FIG. 4. Calculated energy distribution curves for Na at  $\hbar\omega = 5.0$  eV. The ordinate is  $K_G(E)$ , defined in (5.16), and is proportional to  $dI/dE$ . The three cases (a)–(c) correspond to the same labeling in Fig. 3.

face mechanism of photoemission. In order that the interference exist, both matrix elements must exist. They must connect the same initial and final state. For the surface effect one had  $\mathbf{p}_{||} = \mathbf{k}_{i||}$ , while for the volume effect one has  $\mathbf{p}_{||} = \mathbf{k}_{i||} + \mathbf{G}_{||}$ . These can only both be satisfied if  $\mathbf{G}_{||} = 0$ . So there will be interference between the volume effect and the surface effect only for volume-effect optical transitions which have  $\mathbf{G}_{||} = 0$ , or  $\mathbf{G} = G\hat{z}$ .<sup>16</sup> In the case where interference does exist, for  $\lambda a \ll 1$  the resulting term predicts wave-vector conservation in the interband optical transition. So the interference term sends electrons in the same directions as do the pure volume effect transitions for  $\mathbf{G}_{||} = 0$ . For  $\lambda a \ll 1$ , the interference terms are smaller than the volume-effect terms and just slightly alter the intensity of the angular distributions. One cannot evaluate this term without an explicit knowledge of the phase shifts  $\delta(k)$  for the electron wave functions.

## VI. TWO-BAND MODEL

In Sec. V the volume photoemission was calculated with the assumption that the energy bands were completely free-electron-like. That is, the crystal potential was included insofar as it caused interband transitions, but not its corresponding influence upon the shape of the energy bands. Of course, this is inconsistent because the crystal potential causes the bands to distort in the vicinity of the zone edge and at other Bragg planes.

Now we proceed to estimate the influence of this distortion on the external photoemission in the alkali metals. For this we will use a two-band model.<sup>17–19</sup> In the ultraviolet ( $2.0 \leq \hbar\omega \leq 8.0$  eV), the transitions mostly occur near one of the 12 zone faces of the alkali metals. In the two-band model, one diagonalizes exactly the Hamiltonian of the two bands contributing significantly near each of these zone faces. This model has the virtue of simplicity, and it is certainly quite accurate over the photon energy range of interest. One can solve it, and obtain simple expressions for the band structure, the optical absorption, and the angular dependence of external photoemission.

The two-band model has been described before.<sup>17–19</sup> The energies and wave functions near the zone face are

$$E_k^\pm = \frac{1}{2}(\epsilon_k + \epsilon_{k-G}) \pm \left[ \frac{1}{4}(\epsilon_k - \epsilon_{k-G})^2 + V_G^2 \right]^{1/2}, \quad (6.1)$$

$$\psi_k^\pm(\mathbf{r}) = N_k \{ | \epsilon_k - E_k^\mp |^{1/2} \exp(i\mathbf{k} \cdot \mathbf{r}) \pm (V_G / | V_G |) \\ \times | \epsilon_k - E_k^\pm |^{1/2} \exp[i\mathbf{r} \cdot (\mathbf{k} - \mathbf{G})] \}, \quad (6.2)$$

$$N_k = [(\epsilon_k - \epsilon_{k-G})^2 + 4V_G^2]^{-1/4},$$

where  $\mathbf{G}$  is the reciprocal-lattice vector which characterizes that face. Let us warm up to the problem, and gain some appreciation of the amount of band distortion, by calculating the ordinary optical absorption. The imaginary part of the dielectric response

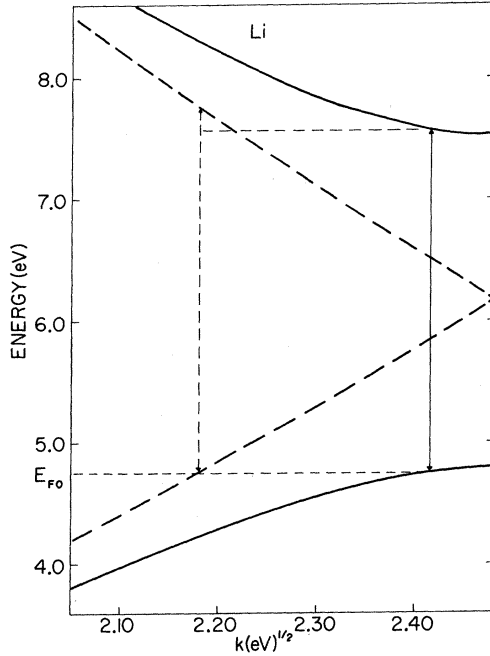


FIG. 5. Energy-band structure for Li along a (110) axis near the zone edge. The dashed lines are the free-electron bands; the solid lines are the two-band-model results. The vertical lines demonstrate that if the Fermi energy  $E_F$  is the same, then the two-band model predicts a lower interband threshold than does the free-electron model.

function is given by the formula

$$\epsilon_2(\omega) = (8\pi^2 e^2 / m^2 \omega^2) \int [d^3k / (2\pi)^3] |\hat{\epsilon} \cdot \langle \psi_{k^+} | \mathbf{p} | \psi_{k^-} \rangle|^2 \times \delta(E_{k^-} + \omega - E_{k^+}).$$

With the wave functions in (6.2) one obtains the matrix element

$$\langle \psi_{k^+} | \hat{\epsilon} \cdot \mathbf{p} | \psi_{k^-} \rangle = \hat{\epsilon} \cdot \mathbf{G} V_G / \omega.$$

Evaluating the integral over wave vectors gives the final result

$$\epsilon_2(\omega) = (e^2 m / \hbar^4 \omega^3) \sum_{\mathbf{G}} [(\hat{\epsilon} \cdot \mathbf{G})^2 V_G^2 / G^3 (\omega^2 - 4V_G^2)^{1/2}] \times (\omega - \omega_1)(\omega_2 - \omega), \quad (6.3)$$

$$\omega_{1,2} = E_G \pm 2[E_G E_F + V_G^2]^{1/2}. \quad (6.4)$$

This reduces to the Wilson-Butcher formula if the crystal potential  $V_G$  is set equal to zero in all of the energy terms.<sup>15</sup> Of course, the Wilson-Butcher formula is derived under the same assumptions used in Sec. V: The influence of the crystal potential is included by its causing interband transitions, but not by its causing band distortions.

Equation (6.4) predicts a result which is in flat contradiction to one's intuition. By comparing it with (5.3), we observe that introducing band gaps and band distortions *lowers the threshold frequency*  $\omega_1$ . This

surprising conclusion is correct if we use the same Fermi energy  $E_F$  in evaluating (5.3) and (6.4). This is illustrated in Fig. 5, where the solid (dashed) vertical line is the threshold with (without) band distortions. At threshold,  $\mathbf{k}$  is parallel to  $\mathbf{G}$ . Fixing  $E_F$  and introducing distortions tends to raise the value of  $k$  at threshold, which overcompensates for the distortion. This difficulty is resolved by noticing that the band distortions must lower the Fermi energy,  $E_F = E_{F0} + \delta E_F$ . An approximate expression for the amount of lowering  $\delta E_F$ , correct to order  $V_G^2$ , is

$$\delta E_F = - \sum_{\mathbf{G}} [V_G^2 / 4(E_{F0} E_G)^{1/2}] \ln(\omega_{20} / \omega_{10}).$$

Values of  $\delta E_F$  are given in Table I.<sup>20</sup> If one uses the adjusted Fermi energy  $E_F = E_{F0} + \delta E_F$  in computing the threshold energies  $\hbar\omega_1$ , then the threshold does become larger than the free-electron value  $\hbar\omega_{10}$ . Of course, the latter value must be computed using  $E_{F0}$ .

The effect on  $\epsilon_2(\omega)$  of this band distortion is shown in Fig. 6. The solid line shows the two-band model result, while the dashed line shows the Wilson-Butcher result. Band-distortion effects are small in Na and K because  $V_G$  has a relatively small value. At this point one can forecast the effects of band distortion on the external photoemission—they are going to be small in Na and K. This conclusion justifies the neglect of such distortions in Sec. V, but it is nonetheless discouraging since such distortions may be used as a measurement of the crystal potential parameter.

Let us proceed with the discussion of the photoemission. Again it is helpful to first see what happens inside the solid in the internal photoemission. Energy

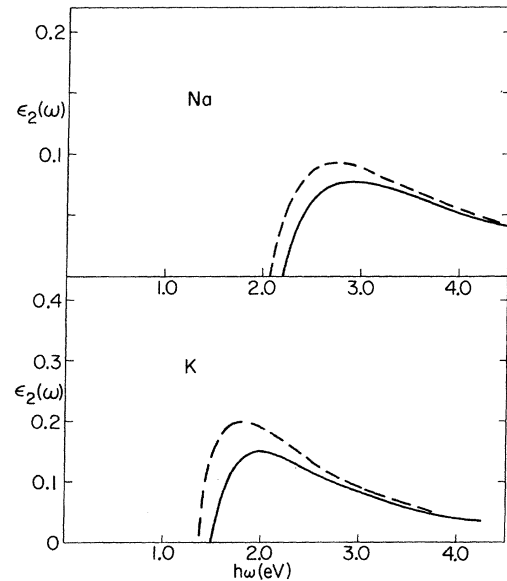


FIG. 6. Interband part of the imaginary part of the dielectric function  $\epsilon_2(\omega)$  for the Wilson-Butcher formula (dashed line) and the two-band model (solid line).

conservation requires that

$$\omega = E_k^+ - E_k^- = [(\epsilon_k - \epsilon_{k-G})^2 + 4V_G^2]^{1/2}. \quad (6.5)$$

Rearranging this equation gives

$$(\omega^2 - 4V_G^2)^{1/2} = \epsilon_k - \epsilon_{k-G} = (KG \cos\theta_0')/m - E_G.$$

Define

$$\Xi = (\omega^2 - 4V_G^2)^{1/2} + E_G \quad (6.6)$$

and we get

$$K^2/2m = \Xi^2/4E_G \cos^2\theta_0'.$$

This differs from (5.1) only in the substitution of  $\Xi$  for  $\Lambda$ . However in this case the energy is not  $K^2/2m$ , but must be derived from (6.1). The final energy, after the interband transition, is

$$E_k^+ = \Xi^2/4E_G \cos^2\theta_0' + \gamma, \\ \gamma = \frac{1}{2}[\omega - (\omega^2 - 4V_G^2)^{1/2}].$$

This is the result which should be compared with (5.1). Again the electrons of a given energy have a conical distribution, where the cone is centered about the direction  $\mathbf{G}$ . This is not surprising when one considers that the energy bands are distorted in the direction of  $\mathbf{G}$ , which is the direction of the cone. So the energy-band distortion only causes the cones of internal electrons to have a slightly different cone angle. But the basic circular symmetry of the cones is maintained. This circular symmetry will only be altered by the energy-band distortion when cones from different  $\mathbf{G}$ 's start to intersect in space. The initial energy of the electrons is given by

$$E_k^- = \Xi^2/4E_G \cos^2\theta_0' - \omega + \gamma.$$

The statement that this initial energy must be less than  $E_F$  leads to the maximum cone angle

$$1 \geq \cos^2\theta_0' \geq \Xi^2/4E_G(E_F + \omega - \gamma).$$

The outer limits of this inequality

$$1 \geq \Xi^2/4E_G(E_F + \omega - \gamma)$$

provides the threshold condition for interband transitions in the two-band model:

$$\omega > \omega_1 = E_G - 2(E_G E_F + V_G^2)^{1/2}.$$

The external photoemission is determined by how these cones are projected outwards through the surface. Again we let  $\mathbf{p} = (\mathbf{p}_\parallel, \mathbf{p}_z)$  be the momentum coordinates outside of the crystal, and  $E = p^2/2m$  be the energy. Inside the crystal, let the wave vector after the interband transition be  $\mathbf{K} = (\mathbf{k}_\parallel, k_z)$ . Conservation of parallel wave vector gives  $\mathbf{k}_\parallel = \mathbf{p}_\parallel$  so that

$$k_\parallel^2 = 2mE \sin^2\theta'.$$

Inside the crystal, after the interband transition, the energy from (6.1) is

$$E_k^+ = E + V_0 = \epsilon_k - \frac{1}{2}(\epsilon_k - \epsilon_{k-G}) + \frac{1}{2}\omega \\ = (k_z^2/2m) + E \sin^2\theta' + \gamma,$$

which may be rearranged to give

$$k_z^2/2m = E \cos^2\theta' + V_0 - \gamma.$$

These two equations determine  $k_\parallel$  and  $k_z$  in terms of  $E$  and  $\theta'$ . They must be inserted into one more equation in order to obtain a result relating  $E$  and  $(\theta', \varphi)$ . This equation is (6.5):

$$\omega = [(\epsilon_k - \epsilon_{k-G})^2 + 4V_G^2]^{1/2},$$

which may be rearranged to give

$$\frac{1}{2}\Xi = (EE_{\parallel})^{1/2} \sin\theta' \cos\varphi + E_z^{1/2}(E \cos^2\theta' + V_0 - \gamma)^{1/2}, \quad (6.7)$$

where  $\Xi$  is given in (6.6). The above result should be compared with the free-electron result (5.3). Equation (6.7) may be solved a number of different ways. The external energy  $E$  may be expressed as a function of the angles  $(\theta', \varphi)$ :

$$E(\theta', \varphi) = (\Xi/2D)^2 \{E_z^{1/2} [\cos^2\theta' - 4D(V_0 - \gamma)/\Xi^2]^{1/2} \\ - E_{\parallel}^{1/2} \sin\theta' \cos\varphi\}^2, \quad (6.8)$$

$$D = E_z \cos^2\theta' - E_{\parallel} \sin^2\theta' \cos^2\varphi.$$

Another result, which is useful for plotting energy contours, is to express  $\theta'$  as a function of  $E$  and  $\varphi$ :

$$\sin\theta' = \Xi \{E_{\parallel}^{1/2} \cos\varphi \\ \pm E_z^{1/2} [4d(E + V_0 - \gamma)/\Xi^2 - 1]^{1/2}\} / 2dE^{1/2}, \quad (6.9)$$

$$d = E_{\parallel} \cos^2\varphi + E_z.$$

Now we are in a position to see how much the directions of the external electrons are affected by the energy-band distortion. The maximum energy at which electrons will come out is still given by

$$E_{\max} = E_F + \omega - V_0.$$

This maximum energy still defines the edge of the cone—the point at which the intensity drops to zero. Since this is a readily measurable quantity, let us see how much this contour of maximum energy is changed by the band distortion. Inside the crystal, let  $\theta_0$  be the free-electron cone angle, and  $\theta_0 + \delta'$  be the cone angle with the band distortions. Outside the crystal, let  $\theta$  be the angle at the free-electron cone edge, and  $\theta + \delta$  be the angle at the cone edge in the two-band model. So  $\delta$  and  $\delta'$  are the shifts in angles caused by the band distortion. Table II shows the values of these parameters for a (100) face of Na and K at  $\hbar\omega = 5.0$  eV. There are essentially two kinds of contributions to  $\delta$  and  $\delta'$ . One is the effect of the actual band distortion, and the second is due to the shift of the Fermi energy caused by this band distortion. The latter effect turns out to be the most significant by a substantial margin. So the angular deviations in Table II really reflect shifts in the Fermi energy rather than the band distortion itself. Angular

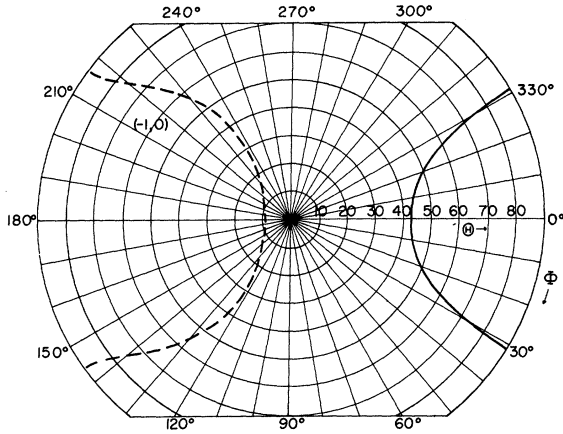


FIG. 7. External distribution of electrons in Na at  $\hbar\omega = 5.0$  eV. The solid line is the primary cone, which is the same curve a Fig. 3(b), while the dashed line is a secondary cone arising from  $G_{||}' = 2\pi(0, -1)/a$ . The lines are the contours of constant energy for  $E_{\text{max}}$ , which defines the outer edge of the cone.

shifts due to the pure distortion are of the order of  $0.1^\circ$  in these metals.

### VII. SECONDARY CONES

So far we have been talking about cones of electrons whose center is at the reciprocal-lattice vector  $\mathbf{G}$  which cooperated in the interband transition. Another effect of band structure is to cause electrons to be emitted in other directions besides these cones. We shall call these other distributions *secondary cones*. These distributions are not conical. They are the distribution obtained by adding a fixed vector onto all of the vectors in the conical distribution. The fixed vector which is added is the parallel component of a reciprocal-lattice vector  $\mathbf{G}_{||}'$ . This is generally not the reciprocal-lattice vector which caused the original interband transition. It is also possible, but irrelevant, that  $\mathbf{G}'$  could be the center of a cone of electrons which it assisted in direct interband transitions.

The crystal potential causes the wave functions to be Bloch functions. These Bloch functions are characterized as being linear combinations of plane waves:

$$\psi_{\mathbf{K}}(\mathbf{r}) = \exp(i\mathbf{K} \cdot \mathbf{r}) \sum_{\mathbf{G}'} u_{\mathbf{K}, \mathbf{G}'} \exp(i\mathbf{G}' \cdot \mathbf{r}). \quad (7.1)$$

In many cases the coefficients  $u_{\mathbf{K}, \mathbf{G}'}$  may be estimated from first-order perturbation theory:

$$u_{\mathbf{K}, \mathbf{G}'} = V_{\mathbf{G}'} / (\epsilon_{\mathbf{K}} - \epsilon_{\mathbf{K} + \mathbf{G}'}).$$

In order to appreciate (7.1), think spatially. It says that a Bloch function is a linear combination of plane waves. So in the interband optical transition, one creates an electron whose wave function has plane-wave components going in these different directions  $\mathbf{K} + \mathbf{G}'$ . So an electron in the state  $\mathbf{K}$  may approach

the surface with the wave vector  $\mathbf{K}$ , but also with  $\mathbf{K} + \mathbf{G}'$ . So electrons will come out of the solid in other directions. These new directions are obtained by matching the wave vector  $\mathbf{K} + \mathbf{G}'$  to the outside components

$$\mathbf{p}_{||} = \mathbf{k}_{||} + \mathbf{G}_{||}'.$$

Of course the energy of the state in the free-electron approximation is still given by  $K^2/2m$ , so that energy conservation still gives that

$$E = p^2/2m = K^2/2m - V_0,$$

or that

$$\begin{aligned} k_z^2 &= p^2 + 2mV_0 - (\mathbf{p}_{||} - \mathbf{G}_{||}')^2 \\ &= p_z^2 + 2mV_0 + 2p_{||}G_{||}' \cos\phi' - G_{||}'^2. \end{aligned}$$

External photoemission only exists if both  $k_z$  and  $p_z$  are real. If one takes their definitions in these above equations, and picks an arbitrary value of  $\mathbf{G}_{||}'$ , he will likely find that one or both of them are complex. These secondary cones only exist for a few selected values of  $\mathbf{G}_{||}'$ , which vary depending upon the initial value of  $\mathbf{G}$  in the transition. Our final equation relates the initial energy of the electron to the final energy. We are still using the convention that the initial wave vector is  $\mathbf{K} - \mathbf{G}$  whereas  $\mathbf{K}$  is the internal wave vector after the interband transition, so that

$$E = (\mathbf{K} - \mathbf{G})^2/2m + \omega - V_0.$$

Rearranging this equation, with the above results for  $k_z$  and  $\mathbf{k}_{||}$ , gives

$$\begin{aligned} \frac{1}{2}\Lambda &= E_z^{1/2} [E \cos^2\theta + V_0 - E_{||}' + 2 \sin\theta \cos\phi' (EE_{||}')^{1/2}]^{1/2} \\ &+ E_{||}'^{1/2} [\sin\theta \cos\phi' E^{1/2} - \cos(\phi - \phi') (E_{||}')^{1/2}], \end{aligned}$$

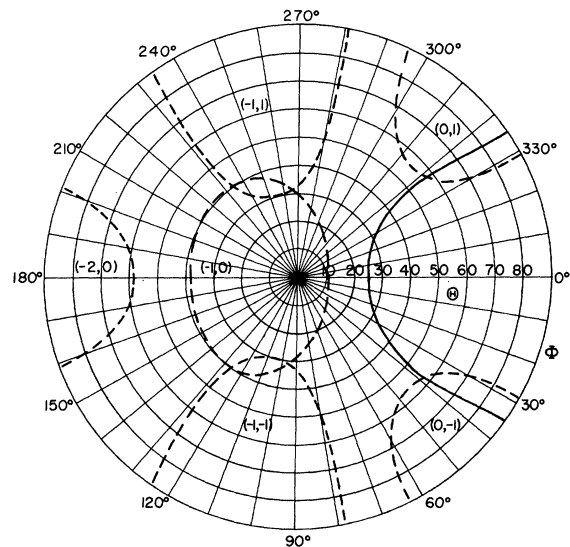


FIG. 8. Same as Fig. 7, except that  $\hbar\omega = 10.0$  eV in Na. There are many secondary cones at this frequency.

where  $\varphi'$  is the angle between  $\mathbf{p}_{||}$  and  $\mathbf{G}_{||}'$ ,  $E_{||}' = G_{||}'^2/2m$ . This equation may be solved to give the external energy as a function of angle:

$$E(\theta, \varphi) = \{B \sin\theta - [B^2 \sin^2\theta + D(\lambda^2 - E_z V_0 + E_z E_{||}')]^{1/2}\}^2 D^{-2},$$

$$\lambda = \frac{1}{2}\Lambda + (E_{||} E_{||}')^{1/2} \cos(\varphi - \varphi'),$$

$$B = \lambda (E_{||})^{1/2} \cos\varphi + E_z (E_{||}')^{1/2} \cos\varphi',$$

or alternatively the angle  $\theta$  as a function of  $E$ ,  $\varphi$ , and  $\varphi'$ :

$$\sin\theta = d(E)^{-1/2} \{B \pm [B^2 - d(\lambda^2 - E_z(V_0 + E - E_{||}'))]^{1/2}\}. \quad (7.2)$$

Figures 7 and 8 show some plots of the external distribution of secondary cones for a (001) face of Na with  $\hbar\omega = 5.0$  eV and 10.0 eV. The solid line in each figure is the contour line of  $E_{\max}$  for the primary cone. The dashed lines are the contour of  $E_{\max}$  for the secondary cones. The primary cone has the components  $G = 2\pi(101)/a$ , and the values of  $G_{||}' = (G_x', G_y')$  for each secondary cone are shown in parentheses. In Fig. 7, at  $\hbar\omega = 5.0$  eV, only one secondary cone is allowed. In Fig. 8, at  $\hbar\omega = 10.0$  eV, many more are present.

#### APPENDIX: INTEGRAL EVALUATION

Many of the results for the external electron current are expressed in terms of integrals over wave vector or angles. These integrals usually contain, as a factor, the surface transmission coefficient  $|T(\mathbf{p}_z, k_z)|^2$ . One needs to know this factor before the integrals may be evaluated. It has a simple form for the model where the surface is a step potential:

$$V(z) = 0, \quad z < 0$$

$$= -V_0, \quad z > 0.$$

Then we get that

$$T(\mathbf{p}_z, k_z) = 2p_z/(k_z + p_z) = (p_z/mV_0)(k_z - p_z).$$

It is possible to evaluate analytically most of the integrals in this paper when this choice is made for  $T(\mathbf{p}_z, k_z)$ . These results will be listed here.

##### A. Surface Effect

1.  $dI/d\Omega$ . From (4.1) and (4.2) we get that ( $\nu = \cos\theta$ )

$$dI/d\Omega = [16e\alpha F(\hat{\mathbf{e}} \cdot \hat{\mathbf{z}})^2 / \pi^2 (\hbar\omega)^3 n V_0] / (1/\nu^3) I_1(\theta, \varphi),$$

$$I_1(\theta, \varphi) = (1/16m^4) \int dk_{iz} p_z^3 k_{iz}^2 [k_z - p_z]^2, \quad (A1)$$

$$k_z = (2m\omega + k_{iz}^2)^{1/2}, \quad p_z = (k_z^2 - 2mV_0)^{1/2}.$$

If we change variables to  $x = p_z/(2m)^{1/2}$ , and define  $x_m^2 = E_{\max} = E_F + \omega - V_0$  and  $x_1 = \max[0, (\omega - V_0)^{1/2}]$ , we get

$$I_1(\theta) = \int_{x_1}^{x_m^2} dx x^4 (x^2 + V_0 - \omega)^{1/2} \times [2x^2 + V_0 - 2x(x^2 + V_0)^{1/2}]. \quad (A2)$$

This integral is a standard form which equals

$$I_1(\theta) = \left\{ \frac{1}{4} x^5 u^3 - (5/24) a u^3 x^3 + \frac{5}{32} a^2 x u^3 - (5/64) a^3 x u \right. \\ \left. + V_0 \left( \frac{1}{8} x^3 u^3 - \frac{1}{8} a x u^3 + \frac{1}{16} a^2 x u \right) \right. \\ \left. + \frac{1}{16} [a^3 V_0 - (5/4) a^4] \ln(x+u) - \frac{1}{4} (x^2 - \frac{5}{8} b) R^3 \right. \\ \left. - \frac{1}{16} (2x^2 + b) [(5/4) b^2 - V_0 a] R \right. \\ \left. + \frac{1}{16} \omega^2 [(5/4) b^2 - a V_0] \ln(u + (x^2 + V_0)^{1/2}) \right\}_{x_1}^{x_m^2},$$

where

$$a = V_0 - \omega, \quad b = 2V_0 - \omega,$$

$$u = (x^2 + a)^{1/2}, \quad R = u(x^2 + V_0)^{1/2}.$$

2.  $I(\omega)$ . From (4.3) and the above results we get

$$I(\omega) = 2\pi \int_0^1 \frac{d\nu}{\nu^3} \int_{x_1}^{x_m^2} dx \{ \dots \}$$

$$= 2\pi \int_{x_1}^{x_m^2} dx \{ \dots \} \int_{(x/x_m)}^1 \frac{d\nu}{\nu^3},$$

where the last step comes from interchanging orders of integration. Evaluating the  $d\nu$  integral yields

$$I(\omega) = \pi \int_{x_1}^{x_m^2} \frac{dx}{x^2} (x_m^2 - x^2) \{ \dots \}.$$

This is the same result obtained by Adawi and others for the total yield. Changing variables to  $y = x^2$  gives

$$I(\omega) = \frac{8e\alpha F(\hat{\mathbf{e}} \cdot \hat{\mathbf{z}})^2}{\pi (\hbar\omega)^3 n V_0} I_2(\omega),$$

$$I_2(\omega) = \int_{y_1}^{y_m} dy y^{1/2} (y_m - y) (y + V_0 - \omega)^{1/2} \times [2y + V_0 - 2y^{1/2}(y + V_0)^{1/2}],$$

$$y_m = E_{\max}, \quad y_1 = \max(0, \omega - V_0).$$

The integral is a standard form which equals

$$I_2 = \left\{ y^{3/2} u^3 \left[ \frac{1}{8} (2y_m - V_0) - \frac{1}{2} (y - \frac{5}{8} a) \right] \right. \\ \left. + \frac{1}{4} \left[ \frac{5}{8} a^2 + \frac{1}{2} a (2y_m - V_0) - V_0 y_m \right] \right. \\ \left. \times [a^2 \ln(y^{1/2} + u) - y^{1/2} u (2y + a)] \right. \\ \left. + u^3 v^3 \left[ \frac{1}{2} y - (5/12) b - \frac{2}{3} y_m \right] - \left[ \frac{5}{8} b^2 - \frac{1}{2} V_0 a + b y_m \right] \right. \\ \left. \times \frac{1}{4} [\omega^2 \ln(u+v) - uv(2y+b)] \right\}_{y_1}^{y_m},$$

$$u = (y+a)^{1/2}, \quad v = (y+V_0)^{1/2}.$$

3.  $dI/dE$ . We get from (4.4)–(4.6)

$$(dI/dE)(E, \omega) = (8/\pi) [e\alpha F(\hat{\mathbf{e}} \cdot \hat{\mathbf{z}})^2 / (\hbar\omega^3) n V_0] I_3,$$

$$I_3 = 2E^{3/2} \int_{\nu_0}^1 d\nu \nu^2 (E\nu^2 + V_0 - \omega)^{1/2} \times [(E\nu^2 + V_0)^{1/2} - \nu E^{1/2}]^2.$$



Changing variables to  $y = E\nu^2$  yields

$$I_3 = \int_{y_1}^E dy y^{1/2} (y + V_0 - \omega)^{1/2} [2y + V_0 - 2y^{1/2}(y + V_0)^{1/2}].$$

This is very similar in form to the integral  $I_2(\omega)$  given above. It equals

$$I_3 = \left\{ \frac{3}{2} u^3 (y^{3/2} - v^3) + \frac{1}{4} u [\omega (2y + a) y^{1/2} - b (2y + b) v^3] - \frac{1}{4} \omega [a^2 \ln(y^{1/2} + u) + \omega b \ln(u + v)] \right\}_{y_1}^E.$$

### B. Volume Effect: $dI/dE$

From (5.16) we get that

$$dI/dE = [e\alpha F l / \pi (\hbar\omega)^3 n] \sum_G [(\hat{\epsilon} \cdot \mathbf{G})^2 / G] V_G^2 K_G(E),$$

$$K_G(E) = \int_0^{2\pi} d\varphi \int_0^1 d\nu J_G(\nu, \varphi) \delta(E - \epsilon(\nu, \varphi)).$$

The quantities  $J_G(\nu = \cos\theta, \varphi)$  and  $\epsilon(\nu, \varphi)$  are defined in (5.4) and (5.13). Now, if  $\mathbf{G}_{||} = 0$ , this gives the simple result (5.18). But, if  $\mathbf{G}_{||} \neq 0$ , we first evaluate the  $d\varphi$  integral to eliminate the  $\delta$  function. After a lengthy bit of algebra, we get, with  $y = [E\nu^2 + V_0]^{1/2}$ ,

$$K_G(E) = \frac{4}{V_0^2} \int_{y_0}^{y_2} y dy \frac{[y^2 - V_0]^{1/2} [y - (y^2 - V_0)^{1/2}]^2}{[(y - y_1)(y_2 - y)]^{1/2}},$$

$$y_2 = \alpha + \beta, \quad y_1 = \alpha - \beta,$$

$$\beta = (E_{||} / E_G)^{1/2} (E + V_0 - \Lambda^2 / 4E_G)^{1/2},$$

$$\alpha = \frac{1}{2} \Lambda E_z^{1/2} / E_G, \quad \gamma = (V_0)^{1/2},$$

and  $y_0$  is the maximum of  $(\gamma, y_1)$ . One has the condition that  $y_2 > y_0$ . This may be reduced by partial

fractions to the form

$$\begin{aligned} K_G(E) = & (2/V_0^2) \left\{ \frac{1}{8} \alpha \gamma [\beta^2 - (\alpha + \gamma)^2] \right. \\ & \times [55\beta^2 + 50\alpha^2 - 29\gamma^2] I_4 \\ & + [\frac{3}{2}\beta^4 + 4\alpha^4 + 12\alpha^2\beta^2 + \gamma^2(\frac{1}{2}\gamma^2 - 2\beta^2 - 4\alpha^2)] I_5 \\ & + [\frac{1}{6}\alpha^2\gamma(55\beta^2 + 50\alpha^2 - 29\gamma^2) \\ & + \frac{1}{3}\alpha\gamma^2(16\beta^2 + 19\alpha^2 - 10\gamma^2)] I_6 \left. \right\} \\ & - (8/V_0^2) \{ [\beta^2 - (y_1 - \alpha)^2]^{1/2} \\ & \times [\frac{1}{4}(\gamma - \alpha)^3 + \frac{4}{3}\alpha(\gamma - \alpha)^2 + \frac{1}{2}(\gamma - \alpha)(\alpha^2 - \gamma^2 + \frac{3}{4}\beta^2) \\ & + 2\alpha(2\alpha^2 - \gamma^2 + \frac{4}{3}\beta^2)] + \cos^{-1}[(y_1 - \alpha)/\beta] \\ & \times [\frac{3}{8}\beta^4 + 3\alpha^2\beta^2 + \alpha^4 - \alpha^2\gamma^2 - \frac{1}{2}\beta^2\gamma^2] \}, \end{aligned}$$

where the elliptic integrals are<sup>21</sup>

$$\begin{aligned} I_4 = & \int_{y_0}^{y_2} dy [(y - \gamma)(y + \gamma)^3 (y - y_1)(y_2 - y)]^{-1/2} \\ & = 2(c + \gamma)^{-1} [(y_2 - c)(y_0 + \gamma)]^{-1/2} \\ & \times \{ K(r) - [(y_2 - c)/(y_2 + \gamma)] E(r) \}, \end{aligned}$$

$$\begin{aligned} I_5 = & \int_{y_0}^{y_2} y dy [(y^2 - \gamma^2)(y_2 - y)(y - y_1)]^{-1/2} \\ & = 2[(y_2 - c)(y_0 + \gamma)]^{-1/2} [(y_2 + \gamma)\pi(s, r) - \gamma K(r)], \end{aligned}$$

$$\begin{aligned} I_6 = & \int_{y_0}^{y_2} dy [(y^2 - \gamma^2)(y_2 - y)(y - y_1)]^{-1/2} \\ & = 2[(y_2 - c)(y_0 + \gamma)]^{-1/2} K(r), \end{aligned}$$

and where

$$c = \min(\gamma, y_1),$$

$$r = [(y_2 - y_0)(c + \gamma) / (y_2 - c)(y_0 + \gamma)]^{1/2},$$

$$s = -(y_2 - y_0) / (y_0 + \gamma).$$

\* Research supported by a National Science Foundation Grant.

† A. P. Sloan Research Fellow.

<sup>1</sup> K. Mitchell, Proc. Roy. Soc. (London) **146A**, 442 (1934).

<sup>2</sup> I. Adawi, Phys. Rev. **134**, A788 (1964).

<sup>3</sup> H. Y. Fan, Phys. Rev. **68**, 43 (1945).

<sup>4</sup> C. N. Berglund and W. E. Spicer, Phys. Rev. **136**, A1030 (1964).

<sup>5</sup> L. Sutton, Phys. Rev. Letters **24**, 386 (1970).

<sup>6</sup> S. Doniach and M. Sunjic, J. Phys. C **3**, 285 (1970).

<sup>7</sup> A preliminary announcement of these results has appeared in G. D. Mahan, Phys. Rev. Letters **24**, 1068 (1970).

<sup>8</sup> N. W. Ashcroft and W. L. Schaich, in *Proceedings of the Density of States Symposium, National Bureau of Standards, 1969* (unpublished).

<sup>9</sup> F. Wooten (private communication).

<sup>10</sup> D. F. DuBois, V. Gilinsky, and M. G. Kivelson, Phys. Rev. **129**, 2376 (1963).

<sup>11</sup> The Ashcroft-Schaich result of Ref. 8 appears formally equivalent to our approach.

<sup>12</sup> J. B. Pendry, J. Phys. C **2**, 2273 (1969).

<sup>13</sup> R. D. Baertsch and J. R. Richardson, J. Appl. Phys. **40**, 229 (1969).

<sup>14</sup> J. Dickey, Phys. Rev. **81**, 612 (1951).

<sup>15</sup> N. V. Smith and W. E. Spicer, Phys. Rev. Letters **23**, 769 (1969).

<sup>16</sup> Ashcroft and Schaich in Ref. 8 obtained interference between the surface and volume effects because they considered this case.

<sup>17</sup> F. S. Ham, Phys. Rev. **128**, 82 (1962); **128**, 2534 (1962).

<sup>18</sup> E.-Ni Foo and J. J. Hopfield, Phys. Rev. **173**, 635 (1968).

<sup>19</sup> G. D. Mahan, J. Res. Natl. Bur. Std. **74A**, 267 (1970).

<sup>20</sup> This predicts an absorption threshold in Li of over 6.0 eV, which is much higher than Ham's value in Ref. 17 or indicated by the experiments: J. N. Hodgson, in *Optical Properties and Electronic Structure of Metals and Alloys*, edited by F. Abeles (Wiley, New York, 1966). Since the value of the Fermi energy is reasonable, the upper band in Li must have a shape quite different than predicted by this two-band model.

<sup>21</sup> P. F. Byrd and M. D. Friedman, *Handbook of Elliptic Integrals for Engineers and Physicists* (Springer-Verlag, Berlin, 1954).